Nitric oxide negatively regulates gibberellin signaling to coordinate growth and salt tolerance in *Arabidopsis*

Lichao Chen,[1,2,3*] Shuhao Sun,[1,2,3] Chun-Peng Song,[4] Jian-Min Zhou[1,2,5], Jiayang Li[1,2,5] and Jianru Zuo[1,2,3,5,6*]

[1]State Key Laboratory of Plant Genomics, Institute of Genetics and Developmental Biology, Chinese Academy of Sciences, Beijing 100101, China. [2]College of Advanced Agricultural Sciences, University of Chinese Academy of Sciences, Beijing 100049, China. [3]CAS Center for Excellence in Molecular Plant Sciences, Chinese Academy of Sciences, Beijing 100101, China. [4] State Key Laboratory of Crop Stress Adaptation and Improvement, Collaborative Innovation Center of Crop Stress Biology, Henan University, Kaifeng 475001, China. [5]Hainan Yazhou Bay Seed Laboratory, Sanya, 572025, China

[6]Lead Contact

*Correspondence: lcchen@genetics.ac.cn amd jrzuo@genetics.ac.cn

Summary

In response to dynamically altered environments, plants must finely coordinate the balance between growth and stress responses for their survival. However, the underpinning regulatory mechanisms remain largely elusive. The phytohormone gibberellin promotes growth via a derepression mechanism by proteasomal degradation of the DELLA transcription repressors. Conversely, the stress-induced burst of nitric oxide (NO) enhances stress tolerance, largely relaying on NO-mediated *S*-nitrosylation, a redox-based posttranslational modification. Here, we show that *S*-nitrosylation of Cys-374 in the *Arabidopsis* RGA protein, a key member of DELLAs, inhibits its interaction with the F-box protein SLY1, thereby preventing its proteasomal degradation under salinity condition. The accumulation of RGA consequently retards growth but enhances salt tolerance . We propose that NO negatively regulates gibberellin signaling via *S*-nitrosylation of RGA to coordinate the balance of growth and stress responses when challenged by adverse environments.

Key words: gibberellin; nitric oxide; *S*-nitrosylation; DELLA repressors; stress responses

INTRODUCTION

To survive under fluctuating environments and unfavorable conditions, plants have evolved sophisticated mechanisms to cope with abiotic and biotic stresses (Zhou and Zhang, 2020; Zhu, 2016). Because available resources are limited and detrimental effects are imposed on plants by stress responses, tradeoff or fine-tuned balance between defense and growth is tightly controlled to allow better fitness for plants (Belda-Palazon et al., 2020; Smakowska et al., 2016; Verma et al., 2016; Yang et al., 2012). However, how plants coordinate growth and stress tolerance is poorly understood.

Phytohormones are key regulators modulating growth and stress tolerance in plants. Among those, gibberellin is a classic growth-promotion phytohormone that regulates a wide range of plant growth and developmental processes, including seed germination, root development, hypocotyl elongation, and flowering (Achard et al., 2007; Debeaujon and Koornneef, 2000; Huang et al., 2010; Shu et al., 2014; Ubeda-Tomas et al., 2008; Wilson et al., 1992). Gibberellin signaling is initiated by binding of the phytohormone to its receptor GA-INSENSITIVE DWARF1 (GID1). The activated GA-GID1 complex interacts with DELLAs to promote their association with the F-box protein SLEEPY1 (SLY1), eventually facilitating the proteasomal degradation of the repressor proteins (Daviere and Achard, 2013; Sun, 2011; Xu et al., 2014). The *Arabidopsis* genome contains a small gene family of 5 members encoding DELLA repressor proteins, namely GA-INSENSITIVE (GAI), REPRESSOR-OF-*ga1-3* (RGA), RGA-LIKE1 (RGL1), RGL2, and RGL3. Among those, *RGA* and *GAI* are major members of this small gene family, as mutations in these two repressors rescue the growth retardation phenotype of *sly1-10* mutant (Dill et al., 2004).

Extensive studies during the past decades have characterized DELLAs as key regulators of gibberellin signaling. DELLAs also act as links to connect with other signaling pathways. Notably, DELLAs physically interact with PHYTOCHROME-INTERACTING FACTOR, BRASSINAZOLE-RESISTANT1, and ETHYLENE INSENSITIVE3, to integrate signals of light

and other phytohormones in coordinating plant growth (Achard et al., 2009; An et al., 2012; Bai et al., 2012; de Lucas et al., 2008; Feng et al., 2008; Ubeda-Tomas et al., 2009). In addition to the modulation of plant growth and development, DELLAs have also been found to regulate stress responses. While DELLA protein SiGAI4 positively regulates cold tolerance in tomato (Wang et al., 2020a) and the *Arabidopsis* gain-of-function mutant *gai-1* displays increased drought tolerance (Wang et al., 2020b), the *Arabidopsis gai-t6 rga-24* double mutant is sensitive to salt treatment (Achard et al., 2006). DELLA proteins also interact with JASMONATE-ZIM DOMAIN (JAZ) to retard the JAZ-MYC2 interaction, thereby enhancing the activity of MYC2 to modulate biotic stress responses (Hou et al., 2010).

Stress responses in plants are more often regulated by the stress-related phytohormones and other signaling molecules, including nitric oxide (NO). As an important signaling molecule, NO plays a vital role in regulating various physiological processes in all living organisms. In plants, NO regulates a wide range of biological processes, including flowering, reproductive development, seed germination, root and shoot development as well as responses to biotic and abiotic stresses (Duan et al., 2020; Fernandez-Marcos et al., 2011; He et al., 2004; Yu et al., 2014). The major bioactive NO species is *S*-nitrosoglutathione (GSNO) that is irreversibly degraded by the highly conserved GSNO reductase (GSNOR) (Liu et al., 2001). In *Arabidopsis*, mutations in the single-copied *GSNOR1* gene cause the accumulation of excessive amount of NO species, resulting in severe defects in development and stress responses (Chen et al., 2009; Feechan et al., 2005; Kwon et al., 2012; Lee et al., 2008). NO executes its physiological effects mainly through protein *S*-nitrosylation, a redox-based posttranslational modification by the addition of an NO molecule to the thiol group of cysteine residue (Cys) to form *S*-nitrosothiol (SNO) (Feng et al., 2019; Hess et al., 2005; Stamler et al., 1992). Protein *S*-nitrosylation modulates diverse functions of proteins, including enzymatic activities, subcellular localization, stability, and protein-protein interactions. In higher plants, mainly in *Arabidopsis*, a number of *S*-nitrosylated proteins have been reported to regulate various developmental processes, immune responses, stress responses, and phytohormone signaling (Astier et al., 2011; Feng et al., 2019;

Yu et al., 2014).

The interplay between NO and phytohormone signaling has been studied in some degrees. In *Arabidopsis*, *S*-nitrosylation of the auxin receptor TIR1 enhances its interaction with the transcriptional repressors Aux/IAA to promote their proteasomal degradation (Terrile et al., 2012). In the cytokinin pathway, while *S*-nitrosylation of a histidine phosphotransfer protein negatively regulates the phosphorelay, leading to a compromised cytokinin response (Feng et al., 2013), NO chemically reacts with cytokinins to regulate the cellular homeostasis of NO (Liu et al., 2013), illustrating a fine-tuned reciprocal regulatory mechanism between these two classes of signaling molecules. In gibberellin signaling, the NO donor sodium nitroprusside (SNP) induces the accumulation of DELLAs (Lozano-Juste and Leon, 2011). Moreover, in response to environmental stress, *S*-nitrosylation of OST1 and ABI5 negatively modulates abscisic acid signaling (Albertos et al., 2015; Wang et al., 2015). These studies highlight the importance of NO-mediated *S*-nitrosylation in regulating both growth and stress responses in plants.

In spite of these efforts, the molecular mechanism regulating the balance between plant growth and stress responses remains largely elusive. In this study, we report that NO induces the *S*-nitrosylation of *Arabidopsis* DELLA protein RGA at Cys-374, which causes the inhibition of the RGA-SLY1 interaction, thereby stabilizing the RGA repressor protein to coordinate plant growth and abiotic stress responses.

Results

Nitric oxide negatively regulates gibberellin signaling via DELLA repressors

Gibberellin mainly promotes plant growth, a biological effect opposite to that of NO. To explore the possible interaction between the NO and gibberellin pathways, we tested the responses of *Arabidopsis* to these two signaling molecules. While gibberellin promoted the elongation of roots and hypocotyls, the NO donor sodium nitroprusside (SNP) inhibited the growth of roots and had no apparent effect on the elongation of hypocotyls (Figure 1A and 1B). The lack of inhibitory effect on hypocotyl elongation is likely attributed to the relatively low concentrations of SNP used in the assay. Nevertheless, SNP antagonized the growth-promotion effect of gibberellin in a dose-dependent manner (Figure 1A and 1B). Treatment with GNSO showed a similar phenotype (Supplemental Figure 1A-1B). Consistent with these observations, the *gsnor1-3* mutant, which accumulates excessive amount of GSNO (Chen et al., 2009; Feechan et al., 2005; Lee et al., 2008), was nearly insensitive to gibberellin for the promotion effect on the elongation of hypocotyls (Figure 1C). Notably, gibberellin reduced the root growth of *gsnor1-3*, a phenotype opposite to that wild type (Figure 1D). These results suggest that NO antagonizes the gibberellin-promoted growth effect.

We reasoned that NO may target DELLA repressor proteins to modulate gibberellin signaling. To test this possibility, we examined the response of mutants carrying various mutations in the *Arabidopsis DELLA* genes to NO. *Arabidopsis* has five *DELLA* genes, of which *RGA* and *GAI* are two major members (Dill et al., 2004; Schwechheimer and Willige, 2009; Xu et al., 2014). Among the analyzed mutants, *rga*, a T-DNA insertion mutant (SALK_089146), carries a null mutation (Supplemental Figure 2A-2C) and *della* is a quadruple mutant carrying null mutations in *RGA*, *GAI*, *RGL1*, and *RGL2* (Cheng et al., 2004). Under normal growth conditions, the *rga* mutant did not have detectable phenotype (Supplemental Figure 2D). However, the *rga* mutant was insensitive to the inhibitory effect of SNP on the elongation of hypocotyls (Figure 1E). Similarly, both the *gai-t6 rga-24* double mutant and *della* quadruple mutant were

hyposensitive to SNP (Figure 1F and 1G). These results suggest that NO negatively regulates gibberellin signaling in a *DELLA*-dependent manner.

Nitric oxide inhibits RGA-SLY1 interaction to stabilize RGA

Data presented above suggest that NO negatively regulates the gibberellin response via *DELLA* genes. We found that the transcription of *RGA* and key gibberellin biosynthesis genes was nearly unaltered when treated with *S*-nitrosoglutathione (GSNO) or SNP (Supplemental Figure 3A-B). Because the gibberellin-induced degradation of DELLA is a key step for the activation of gibberellin signaling, it is reasonable to assume that NO directly or indirectly regulates this class of repressor proteins. We then analyzed the regulation of NO on DELLA proteins. A *pRGA*::*GFP-RGA* transgenic line (Silverstone et al., 2001) was used to analyze the accumulation of RGA protein in response to NO. When treated with GSNO or SNO, the subcellular localization of GFP-RGA did not have detectable alterations (Supplemental Figure 3C). However, the accumulation of GFP-RGA protein was substantially increased by GSNO or SNP in a dose-dependent manner (Figure 2A and Supplemental Figure 3D). A time-course experiment revealed that the accumulation of GFP-RGA was progressively increased upon longer treatment with GSNO or SNP (Figure 2B and Supplemental Figure 3E). Consistent with these observations, the accumulation of RGA protein was significantly higher in NO over-accumulating mutant *gsnor1-3* and *nox1* (He et al., 2004) than that in wild type (Figure 2C), suggesting that NO positively regulates the stability of RGA. Remarkably, the gibberellin-induced degradation of RGA protein was nearly abolished by GSNO or SNP (Figure 2D and Supplemental Figure 3F), suggesting that NO inhibits gibberellin-promoted degradation of RGA protein.

Upon binding to gibberellin, the activated GID1 receptor interacts with DELLA proteins to promote their association with the F-box protein SLY1, thereby facilitating the proteasomal degradation of the repressor proteins. To test if NO regulates the interaction between RGA-GID1 or RGA-SLY1, we performed the following experiments. We found that RGA recombinant protein physically interacted with SLY1 recombinant protein in a pull-down assay and the RGA-

SLY1 interaction was reduced by GSNO in a dose-dependent manner (Figure 2E). A bimolecular fluorescence complementation (BiFC) assay also revealed that NO reduced the RGA-SLY1 interaction *in planta* (Figure 2F). Notably, the RGA-GID1 interaction is not regulated by NO (Supplemental Figure 4A and 4B). Taken together, these results suggest that NO positively regulates the stability of RGA by inhibiting its interaction with the F-box protein SLY1.

_S_-nitrosylation of RGA at Cys-374 inhibits its proteasomal degradation

A major physiological role of NO is executed through protein *S*-nitrosylation. We then asked if RGA was posttranslationally modified by NO. We found that GSNO induced *S*-nitrosylation of RGA recombinant protein in an in vitro biotin-switch assay (Figure 3A). Similarly, GAI, RGL1, RGL2, and RGL3 recombinant proteins were also found being modified by *S*-nitrosylation (Supplemental Figure 5A-5D), suggesting that *S*-nitrosylation plays an important role in regulating DELLA proteins. Moreover, GFP-RGA protein was also found to be S-nitrosylated in planta (Figure 3B). Among 10 Cys residues in RGA, a mass spectrometric analysis of RGA recombinant protein identified Cys-249, Cys-374, Cys-506, and Cys-564 as *S*-nitrosylated residues (Figure 3C and Supplemental Table 1). In two replicates of mass spectrometry, four other Cys residues (Cys-228, Cys-286, Cys-299, and Cys-501) have also been covered, in which no modification was detected. However, Cys-129 and Cys-168 were not covered in mass spectrometry. We could not exclude the possibility that these two Cys residues are modified by *S*-nitrosylation. Because transgenic studies showed that mutations only in Cys-374, but not in Cys-249, Cys-506, and Cys-564, showed detectable effects under stress growth conditions (see below), we focused the analysis of Cys-374 hereafter and the functional studies of other *S*-nitrosylated Cys residues will be published elsewhere. Notably, Cys-374 is conserved in RGA and GAI, but not in other DELLA proteins, suggestive of possible functional divergence of these transcriptional repressors. The substitution of Cys-374 with Ser (RGA^{C374S}) reduced the *S*-nitrosylation of the mutant protein in vitro and in planta (Figure 3D and 3E), indicating that Cys-374 is modified by *S*-nitrosylation.

Because the interaction of RGA with SLY is negatively regulated by NO, we reasoned that the RGA-SLY interaction might be regulated by *S*-nitrosylation. While the RGA-SLY1 interaction was reduced by GSNO, this negative effect was abolished by a RGA^{C374S} mutation in a pull-down assay (Figure 3F). Moreover, the interaction of SLY1 and RGA was detected by a co-immunoprecipitation (Co-IP) assay when transiently expressed in tobacco (*Nicotiana tabacum*) leaves harboring *HA-SLY1* and *FLAG-RGA* or $FLAG\text{-}RGA^{C374S}$ constructs and the interaction was inhibited by SNP. However, SNP exerts NO inhibitory effect on RGA^{C374S}-SLY1 interaction (Fig 3G). Collectively, these results suggest that *S*-nitrosylation at Cys-374 negatively regulates the RGA-SLY1 interaction. Consistent with this observation, the SNP-induced accumulation of GFP-RGA protein was abolished by the RGA^{C374S} mutation (Figure 3H). Moreover, the gibberellin-induced degradation of RGA was inhibited by SNP and GSNO in RGA, but not in RGA^{C374S} mutant proteins (Figure 3I and 3J), suggesting that Cys-374 confers the responsiveness of RGA to NO. These results suggest that *S*-nitrosylation of RGA at Cys-374 inhibits its interaction with the F-box protein SLY1, thereby preventing its proteasomal degradation.

_S_-nitrosylation of RGA at Cys-374 coordinates plant growth and stress responses

Given the importance of *S*-nitrosylation in regulating the stability of RGA, we next explored its physiological significance in modulating growth and stress responses. To this end, a *pRGA*::$GFP\text{-}RGA^{C374S}$ transgene and its control *pRGA*::*GFP-RGA* were introduced into the *gai-t6 rga-24* double mutant by genetic transformation. The *gai-t6 rga-24* double mutant showed elongated hypocotyls and primary roots under normal growth conditions and this phenotype was fully rescued by both *pRGA*::*GFP-RGA* and *pRGA*::$GFP\text{-}RGA^{C374S}$ transgenes (Figure 4A-4C and Supplemental Figure 1B). Moreover, these two transgenes also fully rescued the sensitivity of the *gai-t6 rga-24* double mutant to gibberellin (Figure 4A-4C and Supplemental Figure 1A). However, the response of *gai-t6 rga-24* to SNP and GSNO, regardless of the presence or the absence of gibberellin, was only rescued by *pRGA*::*GFP-RGA*, but not by *pRGA*::$GFP\text{-}RGA^{C374S}$ (Figure 4A-4C, Supplemental Figure 1), consistent with the observation that the accumulation of

RGA, but not RGA^{C374S}, was sensitive to SNP and GSNO (see Figure 3H-3J). These results suggest that *S*-nitrosylation of RGA at Cys-374 plays an important role in regulating gibberellin signaling.

While NO is a key regulator of stress responses (Astier et al., 2011; Feng et al., 2019; Yu et al., 2014), gibberellin signaling is also implied to play a role in salt tolerance, evidenced by the observation that the *gai-t6 rga-24* mutant is hypersensitive to NaCl (Achard et al., 2006). We then asked if *S*-nitrosylation of RGA is involved in regulating stress responses. We found that the hypersensitivity of *gai-t6 rga-24* to NaCl was restored by *pRGA*::*GFP-RGA*, but not by *pRGA*::*GFP-RGA*^{C374S} (Figure 4D-4E). This phenotype was correlated to the accumulation of RGA and RGA^{C374S} proteins in response to NaCl (Figure 4F), in a manner similar to that of SNP (see Figure 3H), suggesting that *S*-nitrosylation of RGA at Cys-374 is essential for its responsiveness to a stress signal. Taken together, these results suggest that *S*-nitrosylation of RGA modulates gibberellin signaling and stress tolerance to coordinate plant growth in response to variable environmental conditions (Figure 4G).

Discussion

In this study, we find that NO negatively regulates gibberellin signaling by stabilizing the RGA repressor via *S*-nitrosylation, which retards growth but positively modulates stress tolerance, thus uncovering a unique mechanism balancing the growth and survival of plants (Figure 4G). While gibberellin is a key regulator promoting plant growth in most, if not all, developmental stages, the burst of NO is generally believed as a hallmark at the onset of stress responses. When challenged by environmental stress, plants usually respond by the inhibition of growth and the activation of stress responses to cope with the detrimental growth conditions. It has been recognized that NO boosts stress tolerance via *S*-nitrosylation of key components of stress responses (Albertos et al., 2015; Hu et al., 2017; Wang et al., 2015; Yang et al., 2015). Also as a protective mechanism, stresses promote the accumulation of DELLA proteins, mediated by decreasing the biosynthesis of gibberellins (Achard et al., 2006; Wang et al., 2020b) or repressing the transcription of *SLY1*, encoding an F-box-containing E3 ligase directly mediating the proteasomal degradation of DELLAs (Lozano-Juste and Leon, 2011), which causes growth inhibition. However, while the inhibitory role of NO on plant growth has been noticed, the underpinning mechanisms remains largely unknown. The finding that *S*-nitrosylation of RGA, a major member of DELLA repressor proteins, inhibits its interaction with SLY1 and consequently prevent its proteasomal degradation, reveals a unique regulatory mechanism that confers plants a more rapid and efficient response when sensing adverse growth conditions. Moreover, we also find that *S*-nitrosylation of RGA at Cys-347 is essential for its regulatory role in salt stress responses. Together, the NO-mediated *S*-nitrosylation of RGA inhibits growth whereas enhances salt stress tolerance, representing a unique mechanism that balances the growth and survival of plants when challenged by detrimental growth conditions.

While an interplay between gibberellin and NO signaling coordinates plant growth and stress responses as revealed in this study, an analogous regulatory scheme has also been appreciated between the cytokinin and NO pathways. The *S*-nitrosylation of AHP1, a key regulator of

cytokinin responses, causes a reduction of its phosphorylation, thereby negatively regulating signaling of this growth-promotion phytohormone (Feng et al., 2013). Therefore, *S*-nitrosylation may represent an important mechanism that integrates an NO signal into signaling of growth-promotion phytohormones and eventually retards growth in response to environmental stresses. It has been noticed that the protein *S*-nitrosylation level is tightly regulated by the intracellular NO concentrations (Benhar et al., 2009; Feng et al., 2019; Hess et al., 2005; Hu et al., 2015), which is induced by various stimuli in fluctuating environments (Wang et al., 2010; Zhao et al., 2009; Zhou et al., 2016). Thus, *S*-nitrosylation of DELLA proteins permits a rapid response to diverse environmental alterations. When growth conditions become favorable, the intracellular NO level is returned to a physiologically normal level, which may trigger a reverse denitrosylation reaction (Benhar et al., 2009; Kneeshaw et al., 2014; Tada et al., 2008). It is reasonable to speculate that the denitrosylation of RGA resets the transcriptional repressor under the control of gibberellin-promoted proteasomal degradation, thereby relieving from the growth retardation. Therefore, RGA acts a signaling molecule to sense intracellular NO level to coordinate plant growth and stress tolerance in response to dynamically altered environment.

In addition to Cys-374, several other Cys residues, including Cys-249, Cys-506, and Cys-564, of RGA are also identified as the *S*-nitrosylated sites in mass spectrometric analysis. While *S*-nitrosylation of these Cys residues remains functionally unclear, it is well known that gibberellins regulate multiple biological processes, largely dependent on the interactions between DELLAs and transcription factors of other signaling pathways. For instance, GAI and RGA interact physically with PIF3 and PIF4, two bHLH transcription factors, to regulates the plant growth (de Lucas et al., 2008; Feng et al., 2008). As NO is invovled in regulating diverse biological processes, it is of great interest to investigate whether *S*-nitrosylation at Cys-249, Cys-506, or Cys-564 affects interaction between RGA and its interacting proteins.

Finally, DELLA proteins are regulated by multiple forms of posttranslational modifications, including phosphorylation, SUMOylation, *O*-GlcNAcylation, and *O*-fucosylation (Conti et al., 2014; Dai and Xue, 2010; Zentella et al., 2016). Investigation of possible interactions of these

289 posttranslational modifications, including *S*-nitrosylation, will be of great interests toward the
290 understanding how plants balance growth and stress tolerance in response to environmental
291 alterations.
292

STAR★METHODS

Detailed methods are provided in the online version of this paper and include the following:

- **KEY RESOURCES TABLE**
- **LEAD CONTACT AND MATERIALS AVAILABILITY**
- **EXPERIMENTAL MODEL AND SUBJECT DETAILS**
- **METHOD DETAILS**
  - Plasmid construction
  - Expression and purification of recombinant proteins
  - Generation of antibodies and immunoblotting
  - Bimolecular fluorescence complementation analyses
  - In vitro pull down
  - Co-immunoprecipitation
  - In vitro *S*-nitrosylation assay
  - In vivo *S*-nitrosylation assay
  - Mass spectrometric analysis of *S*-nitrosylation residues

- **QUANTIFICATION AND STATISTICAL ANALYSIS**
- **DATA AND CODE AVAILABILITY**

SUPPLEMENTAL INFORMATION

Supplemental information includes 5 figures and 2 tables and can be found with this article online.

ACKNOWLEDGEMENTS

We thank the *Arabidopsis* Biological Resource Center (ABRC) and Xiangdong Fu for seeds. This work was supported by grants from the National Natural Science Foundation of China (31830017 and 31521001), Chinese Academy of Sciences (XDB27030207), and State Key Laboratory of

Plant Genomics (SKLPG2020-22).

AUTHOR CONTRIBUTIONS

L.C. performed the majority of the experiment, assisted by S.S. J.Z., L.C., J.-M.Z., and JL designed the experiments and analyzed the data. J.Z. wrote the manuscript, assisted by L.C. All authors discussed the results and commented on the manuscript.

DECLARATION OF INTEREST

The authors declare no competing interests.

Reference

Achard, P., Cheng, H., De Grauwe, L., Decat, J., Schoutteten, H., Moritz, T., Van Der Straeten, D., Peng, J., and Harberd, N.P. (2006). Integration of plant responses to environmentally activated phytohormonal signals. Science *311*, 91-94.

Achard, P., Gusti, A., Cheminant, S., Alioua, M., Dhondt, S., Coppens, F., Beemster, G.T., and Genschik, P. (2009). Gibberellin signaling controls cell proliferation rate in Arabidopsis. Curr Biol *19*, 1188-1193.

Achard, P., Liao, L., Jiang, C., Desnos, T., Bartlett, J., Fu, X., and Harberd, N.P. (2007). DELLAs contribute to plant photomorphogenesis. Plant Physiol *143*, 1163-1172.

Albertos, P., Romero-Puertas, M.C., Tatematsu, K., Mateos, I., Sanchez-Vicente, I., Nambara, E., and Lorenzo, O. (2015). S-nitrosylation triggers ABI5 degradation to promote seed germination and seedling growth. Nat Commun *6*, 8669.

An, F., Zhang, X., Zhu, Z., Ji, Y., He, W., Jiang, Z., Li, M., and Guo, H. (2012). Coordinated regulation of apical hook development by gibberellins and ethylene in etiolated Arabidopsis seedlings. Cell Res *22*, 915-927.

Astier, J., Rasul, S., Koen, E., Manzoor, H., Besson-Bard, A., Lamotte, O., Jeandroz, S., Durner, J., Lindermayr, C., and Wendehenne, D. (2011). S-nitrosylation: an emerging post-translational protein modification in plants. Plant Sci *181*, 527-533.

Bai, M.Y., Shang, J.X., Oh, E., Fan, M., Bai, Y., Zentella, R., Sun, T.P., and Wang, Z.Y. (2012). Brassinosteroid, gibberellin and phytochrome impinge on a common transcription module in Arabidopsis. Nat Cell Biol *14*, 810-817.

Bechtold, N., and Pelletier, G. (1998). In planta Agrobacterium-mediated transformation of adult Arabidopsis thaliana plants by vacuum infiltration. Methods Mol Biol *82*, 259-266.

Belda-Palazon, B., Adamo, M., Valerio, C., Ferreira, L.J., Confraria, A., Reis-Barata, D., Rodrigues, A., Meyer, C., Rodriguez, P.L., and Baena-Gonzalez, E. (2020). A dual function of SnRK2 kinases in the regulation of SnRK1 and plant growth. Nat Plants *6*, 1345-1353.

Benhar, M., Forrester, M.T., and Stamler, J.S. (2009). Protein denitrosylation: enzymatic mechanisms and cellular

355 functions. Nat Rev Mol Cell Biol *10*, 721-732.
356 Chen, L., Wu, R., Feng, J., Feng, T., Wang, C., Hu, J., Zhan, N., Li, Y., Ma, X., Ren, B.*, et al.* (2020).
357 Transnitrosylation Mediated by the Non-canonical Catalase ROG1 Regulates Nitric Oxide Signaling in Plants. Dev
358 Cell *53*, 444-457 e445.
359 Chen, R.Q., Sun, S.L., Wang, C., Li, Y.S., Liang, Y., An, F.Y., Li, C., Dong, H.L., Yang, X.H., Zhang, J.*, et al.* (2009).
360 The Arabidopsis PARAQUAT RESISTANT2 gene encodes an S-nitrosoglutathione reductase that is a key regulator
361 of cell death. Cell Research *19*, 1377-1387.
362 Cheng, H., Qin, L., Lee, S., Fu, X., Richards, D.E., Cao, D., Luo, D., Harberd, N.P., and Peng, J. (2004). Gibberellin
363 regulates Arabidopsis floral development via suppression of DELLA protein function. Development *131*, 1055-1064.
364 Conti, L., Nelis, S., Zhang, C., Woodcock, A., Swarup, R., Galbiati, M., Tonelli, C., Napier, R., Hedden, P., Bennett,
365 M.*, et al.* (2014). Small Ubiquitin-like Modifier protein SUMO enables plants to control growth independently of the
366 phytohormone gibberellin. Dev Cell *28*, 102-110.
367 Dai, C., and Xue, H.W. (2010). Rice early flowering1, a CKI, phosphorylates DELLA protein SLR1 to negatively
368 regulate gibberellin signalling. EMBO J *29*, 1916-1927.
369 Daviere, J.M., and Achard, P. (2013). Gibberellin signaling in plants. Development *140*, 1147-1151.
370 de Lucas, M., Daviere, J.M., Rodriguez-Falcon, M., Pontin, M., Iglesias-Pedraz, J.M., Lorrain, S., Fankhauser, C.,
371 Blazquez, M.A., Titarenko, E., and Prat, S. (2008). A molecular framework for light and gibberellin control of cell
372 elongation. Nature *451*, 480-484.
373 Debeaujon, I., and Koornneef, M. (2000). Gibberellin requirement for Arabidopsis seed germination is determined
374 both by testa characteristics and embryonic abscisic acid. Plant Physiology *122*, 415-424.
375 Dill, A., Thomas, S.G., Hu, J., Steber, C.M., and Sun, T.P. (2004). The Arabidopsis F-box protein SLEEPY1 targets
376 gibberellin signaling repressors for gibberellin-induced degradation. Plant Cell *16*, 1392-1405.
377 Duan, Q., Liu, M.J., Kita, D., Jordan, S.S., Yeh, F.J., Yvon, R., Carpenter, H., Federico, A.N., Garcia-Valencia, L.E.,
378 Eyles, S.J.*, et al.* (2020). FERONIA controls pectin- and nitric oxide-mediated male-female interaction. Nature *579*,
379 561-566.
380 Feechan, A., Kwon, E., Yun, B.W., Wang, Y., Pallas, J.A., and Loake, G.J. (2005). A central role for S-nitrosothiols in
381 plant disease resistance. Proc Natl Acad Sci U S A *102*, 8054-8059.
382 Feng, J., Chen, L., and Zuo, J. (2019). Protein S-Nitrosylation in plants: Current progresses and challenges. J Integr
383 Plant Biol *61*, 1206-1223.
384 Feng, J., Wang, C., Chen, Q., Chen, H., Ren, B., Li, X., and Zuo, J. (2013). S-nitrosylation of phosphotransfer
385 proteins represses cytokinin signaling. Nature Communications *4*, 1529.
386 Feng, S., Martinez, C., Gusmaroli, G., Wang, Y., Zhou, J., Wang, F., Chen, L., Yu, L., Iglesias-Pedraz, J.M., Kircher,
387 S.*, et al.* (2008). Coordinated regulation of Arabidopsis thaliana development by light and gibberellins. Nature *451*,
388 475-479.
389 Fernandez-Marcos, M., Sanz, L., Lewis, D.R., Muday, G.K., and Lorenzo, O. (2011). Nitric oxide causes root apical
390 meristem defects and growth inhibition while reducing PIN-FORMED 1 (PIN1)-dependent acropetal auxin transport.
391 Proc Natl Acad Sci U S A *108*, 18506-18511.
392 He, Y., Tang, R.H., Hao, Y., Stevens, R.D., Cook, C.W., Ahn, S.M., Jing, L., Yang, Z., Chen, L., Guo, F.*, et al.*
393 (2004). Nitric oxide represses the Arabidopsis floral transition. Science *305*, 1968-1971.
394 Hess, D.T., Matsumoto, A., Kim, S.O., Marshall, H.E., and Stamler, J.S. (2005). Protein S-nitrosylation: purview and
395 parameters. Nat Rev Mol Cell Biol *6*, 150-166.

Hou, X., Lee, L.Y., Xia, K., Yan, Y., and Yu, H. (2010). DELLAs modulate jasmonate signaling via competitive binding to JAZs. Dev Cell *19*, 884-894.

Hu, J., Huang, X., Chen, L., Sun, X., Lu, C., Zhang, L., Wang, Y., and Zuo, J. (2015). Site-specific nitrosoproteomic identification of endogenously S-nitrosylated proteins in Arabidopsis. Plant Physiol *167*, 1731-1746.

Hu, J., Yang, H., Mu, J., Lu, T., Peng, J., Deng, X., Kong, Z., Bao, S., Cao, X., and Zuo, J. (2017). Nitric Oxide Regulates Protein Methylation during Stress Responses in Plants. Mol Cell *67*, 702-710 e704.

Huang, J., Tang, D., Shen, Y., Qin, B., Hong, L., You, A., Li, M., Wang, X., Yu, H., Gu, M.*, et al.* (2010). Activation of gibberellin 2-oxidase 6 decreases active gibberellin levels and creates a dominant semi-dwarf phenotype in rice (Oryza sativa L.). J Genet Genomics *37*, 23-36.

King, K.E., Moritz, T., and Harberd, N.P. (2001). Gibberellins are not required for normal stem growth in Arabidopsis thaliana in the absence of GAI and RGA. Genetics *159*, 767-776.

Kneeshaw, S., Gelineau, S., Tada, Y., Loake, G.J., and Spoel, S.H. (2014). Selective protein denitrosylation activity of Thioredoxin-h5 modulates plant Immunity. Mol Cell *56*, 153-162.

Kwon, E., Feechan, A., Yun, B.W., Hwang, B.H., Pallas, J.A., Kang, J.G., and Loake, G.J. (2012). AtGSNOR1 function is required for multiple developmental programs in Arabidopsis. Planta *236*, 887-900.

Lee, U., Wie, C., Fernandez, B.O., Feelisch, M., and Vierling, E. (2008). Modulation of nitrosative stress by S-nitrosoglutathione reductase is critical for thermotolerance and plant growth in Arabidopsis. Plant Cell *20*, 786-802.

Liu, L., Hausladen, A., Zeng, M., Que, L., Heitman, J., and Stamler, J.S. (2001). A metabolic enzyme for S-nitrosothiol conserved from bacteria to humans. Nature *410*, 490-494.

Liu, W.Z., Kong, D.D., Gu, X.X., Gao, H.B., Wang, J.Z., Xia, M., Gao, Q., Tian, L.L., Xu, Z.H., Bao, F.*, et al.* (2013). Cytokinins can act as suppressors of nitric oxide in Arabidopsis. Proc Natl Acad Sci U S A *110*, 1548-1553.

Lozano-Juste, J., and Leon, J. (2011). Nitric oxide regulates DELLA content and PIF expression to promote photomorphogenesis in Arabidopsis. Plant Physiol *156*, 1410-1423.

Ren, B., Chen, Q., Hong, S., Zhao, W., Feng, J., Feng, H., and Zuo, J. (2013). The *Arabidopsis* eukaryotic translation initiation factor eIF5A-2 regulates root protoxylem development by modulating cytokinin signaling. Plant Cell *25*, 3841-3857.

Schwechheimer, C., and Willige, B.C. (2009). Shedding light on gibberellic acid signalling. Curr Opin Plant Biol *12*, 57-62.

Shu, K., Wu, Y., Yang, W., and Xie, Q. (2014). Concurrent deficiency of gibberellins and abscisic acid causes plant male sterility. J Genet Genomics *41*, 601-604.

Silverstone, A.L., Jung, H.S., Dill, A., Kawaide, H., Kamiya, Y., and Sun, T.P. (2001). Repressing a repressor: gibberellin-induced rapid reduction of the RGA protein in Arabidopsis. Plant Cell *13*, 1555-1566.

Smakowska, E., Kong, J., Busch, W., and Belkhadir, Y. (2016). Organ-specific regulation of growth-defense tradeoffs by plants. Curr Opin Plant Biol *29*, 129-137.

Stamler, J.S., Simon, D.I., Osborne, J.A., Mullins, M.E., Jaraki, O., Michel, T., Singel, D.J., and Loscalzo, J. (1992). S-nitrosylation of proteins with nitric oxide: synthesis and characterization of biologically active compounds. Proc Natl Acad Sci U S A *89*, 444-448.

Sun, T.P. (2011). The molecular mechanism and evolution of the GA-GID1-DELLA signaling module in plants. Curr Biol *21*, R338-345.

Tada, Y., Spoel, S.H., Pajerowska-Mukhtar, K., Mou, Z., Song, J., Wang, C., Zuo, J., and Dong, X. (2008). Plant immunity requires conformational changes of NPR1 via S-nitrosylation and thioredoxins. Science *321*, 952-956.

Terrile, M.C., Paris, R., Calderon-Villalobos, L.I., Iglesias, M.J., Lamattina, L., Estelle, M., and Casalongue, C.A. (2012). Nitric oxide influences auxin signaling through S-nitrosylation of the Arabidopsis TRANSPORT INHIBITOR RESPONSE 1 auxin receptor. Plant Journal *70*, 492-500.

Ubeda-Tomas, S., Federici, F., Casimiro, I., Beemster, G.T., Bhalerao, R., Swarup, R., Doerner, P., Haseloff, J., and Bennett, M.J. (2009). Gibberellin signaling in the endodermis controls Arabidopsis root meristem size. Curr Biol *19*, 1194-1199.

Ubeda-Tomas, S., Swarup, R., Coates, J., Swarup, K., Laplaze, L., Beemster, G.T.S., Hedden, P., Bhalerao, R., and Bennett, M.J. (2008). Root growth in Arabidopsis requires gibberellin/DELLA signalling in the endodermis. Nat Cell Biol *10*, 625-628.

Verma, V., Ravindran, P., and Kumar, P.P. (2016). Plant hormone-mediated regulation of stress responses. BMC Plant Biol *16*, 86.

Wang, F., Chen, X., Dong, S., Jiang, X., Wang, L., Yu, J., and Zhou, Y. (2020a). Crosstalk of PIF4 and DELLA modulates CBF transcript and hormone homeostasis in cold response in tomato. Plant Biotechnol J *18*, 1041-1055.

Wang, P., Du, Y., Hou, Y.J., Zhao, Y., Hsu, C.C., Yuan, F., Zhu, X., Tao, W.A., Song, C.P., and Zhu, J.K. (2015). Nitric oxide negatively regulates abscisic acid signaling in guard cells by S-nitrosylation of OST1. Proc Natl Acad Sci U S A *112*, 613-618.

Wang, P., Du, Y., Li, Y., Ren, D., and Song, C.P. (2010). Hydrogen peroxide-mediated activation of MAP kinase 6 modulates nitric oxide biosynthesis and signal transduction in Arabidopsis. Plant Cell *22*, 2981-2998.

Wang, Z., Liu, L., Cheng, C., Ren, Z., Xu, S., and Li, X. (2020b). GAI Functions in the Plant Response to Dehydration Stress in Arabidopsis thaliana. Int J Mol Sci *21*.

Wilson, R.N., Heckman, J.W., and Somerville, C.R. (1992). Gibberellin Is Required for Flowering in Arabidopsis-Thaliana under Short Days. Plant Physiology *100*, 403-408.

Xu, H., Liu, Q., Yao, T., and Fu, X. (2014). Shedding light on integrative GA signaling. Curr Opin Plant Biol *21*, 89-95.

Yang, D.L., Yao, J., Mei, C.S., Tong, X.H., Zeng, L.J., Li, Q., Xiao, L.T., Sun, T.P., Li, J., Deng, X.W.*, et al.* (2012). Plant hormone jasmonate prioritizes defense over growth by interfering with gibberellin signaling cascade. Proc Natl Acad Sci U S A *109*, E1192-1200.

Yang, H., Mu, J., Chen, L., Feng, J., Hu, J., Li, L., Zhou, J.M., and Zuo, J. (2015). S-nitrosylation positively regulates ascorbate peroxidase activity during plant stress responses. Plant Physiol *167*, 1604-1615.

Yu, M., Lamattina, L., Spoel, S.H., and Loake, G.J. (2014). Nitric oxide function in plant biology: a redox cue in deconvolution. New Phytol *202*, 1142-1156.

Zentella, R., Hu, J., Hsieh, W.P., Matsumoto, P.A., Dawdy, A., Barnhill, B., Oldenhof, H., Hartweck, L.M., Maitra, S., Thomas, S.G.*, et al.* (2016). O-GlcNAcylation of master growth repressor DELLA by SECRET AGENT modulates multiple signaling pathways in Arabidopsis. Genes Dev *30*, 164-176.

Zhao, M.G., Liu, R.J., Chen, L., Tian, Q.Y., and Zhang, W.H. (2009). Glucose-induced inhibition of seed germination in Lotus japonicus is alleviated by nitric oxide and spermine. J Plant Physiol *166*, 213-218.

Zhou, J.M., and Zhang, Y. (2020). Plant Immunity: Danger Perception and Signaling. Cell *181*, 978-989.

Zhou, S., Jia, L., Chu, H., Wu, D., Peng, X., Liu, X., Zhang, J., Zhao, J., Chen, K., and Zhao, L. (2016). Arabidopsis CaM1 and CaM4 Promote Nitric Oxide Production and Salt Resistance by Inhibiting S-Nitrosoglutathione Reductase via Direct Binding. PLoS Genet *12*, e1006255.

Zhu, J.K. (2016). Abiotic Stress Signaling and Responses in Plants. Cell *167*, 313-324.

478 Zuo, J.R., Niu, Q.W., and Chua, N.H. (2000). An estrogen receptor-based transactivator XVE mediates highly
479 inducible gene expression in transgenic plants. Plant Journal *24*, 265-273.

480

481

FIGURE LEGENDS

Figure 1. Nitric oxide antagonizes gibberellin-p romoted root and hypocotyl elongation, see also Supplemental Figure S1 and S2

(A and B) Hypocotyl length (A) and primary root length (B) of 7-day-old Col-0 seedlings treated with the indicated concentrations of gibberellic acid (GA_3) and sodium nitroprusside (SNP).

(C and D) Hypocotyl length (C) and primary root length (D) of 7-day-old Col-0 and *gsnor1-3* seedlings treated with 5 μM GA_3.

(E) Hypocotyl length of 7-day-old Col-0 and *rga* seedlings treated with 20 μM SNP.

(F and G) Hypocotyl length (F) and primary root length (G) of 7-day-old Col-0, *gai-t6 rga-24* and *della* (*gai-t6 rga-t2 rgl1-1 rgl2-1*) seedlings treated with 20 μM SNP.

In each experiment, 30 seedlings were analyzed. *, **, and *** indicate $P < 0.05$, $P < 0.01$, and $P < 0.001$ (one-way ANOVA test), respectively.

Figure 2. Nitric oxide inhibits gibberellin-promoted RGA degradation, see also Supplemental Figure S3, S4 and Table S1

(A and B) Immunoblotting analysis of GFP-RGA proteins in 7-day-old *pRGA*::*GFP-RGA* transgenic seedlings treated with indicated concentrations of GSNO for 6 hours (A) and 300 μM GSNO for the indicated times (B) by using an anti-GFP antibody. Immunoblotting with an anti-tubulin antibody is served as a loading control. Quantification of GFP-RGA is shown below the blot.

(C) Immunoblotting analysis of RGA proteins in 7-day-old Col-0, *gsnor1-3*, and *nox1* seedlings by using an anti-RGA antibody. Quantification of RGA is shown below the blot.

(D) Immunoblotting analysis of GFP-RGA proteins in 7-day-old *pRGA*::*GFP-RGA* transgenic seedlings treated with or without 300 μM GSNO and 0.5 μM GA_3 for 6 hours using an anti-GFP antibody. Quantification of GFP-RGA is shown below the blot.

(E) Analysis of the interaction of SLY1 and RGA1 recombinant proteins with a pull-down assay.

GST^{4CS}-RGA protein was treated with the indicated concentrations of GSNO or GSH prior to the incubation with His-SLY1. Quantification of the His-SLY1 level is shown below the blot.

(F) Bimolecular fluorescence complementation (BiFC) analysis of co-localization of YNE-RGA1 and YCE-SLY1 fusion proteins in transiently expressed in tobacco leaves sprayed with 300 μM GSNO. Bar, 20 μm.

Figure 3. *S*-nitrosylation at Cys-374 modulates RGA stability, see also Supplemental Figure S5, Table S1 and Table S2

(A) Analysis of *S*-nitrosylated GST^{4CS}-RGA recombinant protein treated with GSNO by an in vitro *S*-nitrosylation assay. Treatment with GSH and without sodium ascorbate (Asc) are served as negative controls.

(B) Analysis of *S*-nitrosylated GFP-RGA protein in *pRGA*::*GFP-RGA* transgenic seedlings by an in vivo *S*-nitrosylation assay. The sample without Asc treatment is served as a negative control.

(C) Liquid chromatography tandem-mass (LC-MS/MS) spectrum of trypsin-digested and biotin-charged RGA peptides. The b- and y-type product ions are indicated, which identified Cys-374 as an *S*-nitrosylated residue.

(D) Analysis of *S*-nitrosylated GST^{4CS}-RGA (RGA) and GST^{4CS}-RGA^{C374S} (C374S) recombinant proteins treated with GSNO by an in vitro *S*-nitrosylation assay. Treatment with GSH is served as negative controls. Quantification of the *S*-nitrosylation level of GST^{4CS}-RGA and GST^{4CS}-RGA^{C374S} is shown below the blot.

(E) Analysis of *S*-nitrosylated GFP-RGA and RGA^{C374S} (C374S) proteins in planta by an in vivo *S*-nitrosylation assay. The sample without Asc treatment is served as a negative control. Quantification of the *S*-nitrosylation level of RGA and RGA^{C374S} is shown below the blot.

(F) Analysis of the interaction of RGA, RGA^{C374S} and SLY1 recombinant proteins with a pull-down assay. GST^{4CS}-RGA and GST^{4CS}-RGA^{C374S} was treated with 300 μM GSNO to generate *S*-nitrosylated proteins prior to the incubation with His-SLY1.

(G) Analysis of the interaction of HA-SLY1, FLAG-RGA and FLAG-RGA^{C374S} (FLAG-C374S) proteins by a co-immunoprecipitation assay. The *HA-SLY1* and *FLAG-RGA* fusion genes under

537 the control of the 35S promoter were transiently expressed in tobacco leaves that were incubated
538 with or without 300 μM SNP for 1 hour. Protein extracts were used for Co-IP and analyzed by
539 immunoblotting using anti-HA and -FLAG antibodies. Quantification of HA-SLY1 is shown
540 below the blot. And protein level of HA-SLY1 that interacts with FLAG-RGA and FLAG-C374S
541 without SNP treatment is set as 1.0, respectively.
542 (H) Immunoblotting analysis of GFP-RGA proteins in *gai-t6 rga-24* transgenic seedlings of the
543 indicated genotypes treated with 300 μM SNP for 6 hours using an anti-RGA antibody.
544 Quantification of the GFP-RGA and GFP-RGA^{C374S} protein levels is shown below the blot.
545 Protein levels of GFP-RGA and GFP-RGA^{C374S} without treatment are set as 1.0, respectively.
546 (I) Immunoblotting analysis of GFP-RGA and GFP-RGA^{C374S} proteins in 7-day-old *pRGA*::*GFP-*
547 *RGA*, *pRGA*::*GFP-RGA*^{C374S} transgenic seedlings treated with or without 300 μM GSNO and 0.5
548 μM GA_3 for 6 hours by using an anti-RGA antibody. Quantification of the GFP-RGA and GFP-
549 RGA^{C374S} protein levels is shown below the blot. Protein levels of GFP-RGA and GFP-
550 RGAC374S without treatment are set as 1.0, respectively.
551 (J) Immunoblotting analysis of GFP-RGA and GFP-RGA^{C374S} proteins in 7-day-old *pRGA*::*GFP-*
552 *RGA*, *pRGA*::*GFP-RGA*^{C374S} transgenic seedlings treated with or without 300 μM SNP, and 0.5
553 μM GA_3 for 6 hours by using an anti-RGA antibody. Quantification of the GFP-RGA and GFP-
554 RGA^{C374S} protein levels is shown below the blot. Protein levels of GFP-RGA and GFP-RGA^{C374S}
555 without treatment are set as 1.0, respectively.
556 Data presented in (H)-(J) are means of three independent experiments with S.D. * and ** indicate
557 $P < 0.05$ and $P < 0.01$, respectively (One-way ANOVA test).
558
559 **Figure 4. *S*-nitrosylation of RGA balances plant growth and salinity tolerance, see also**
560 **Figure S1 and Supplemental Table S1**
561 (A) Ten-day-old seedlings of the indicated genotypes treated with 50 μM SNP or 5 μM GA_3. Bar,
562 1 cm.
563 (B) and (C) Analysis of hypocotyl length (B) and primary root length (C) of transgenic seedlings

564 of the indicated genotypes treated with 50 μM SNP or 5 μM GA_3 for 10 days.
565 (D) Five-day-old seedlings of the indicated genotypes on 1/2MS medium were transferred to the
566 medium containing 125 mM NaCl. Photos were taken 2 weeks post the transfer. Bar, 1 cm.
567 (E) Analysis of the survival rate of transgenic seedlings of the indicated genotypes shown in (D).
568 (F) Immunoblotting analysis of GFP-RGA proteins in *gai-t6 rga-24* transgenic seedlings of the
569 indicated genotypes treated with 150 mM NaCl for 6 hours using an anti-RGA antibody.
570 Quantification of the GFP-RGA and GFP-RGA^{C374S} protein levels is shown below the blot.
571 (G) A proposed model illustrating the function of *S*-nitrosylation of RGA. Under normal growth
572 conditions, SLY1 interacts with RGA, which leads to the polyubiquitination and degradation of
573 RGA via the 26S proteasome pathway. High salt induces the NO burst, which subsequently
574 induces the *S*-nitrosylation of RGA. The *S*-nitrosylation inhibits the RGA-SLY1 interaction and
575 enhances the stability of RGA. Accumulating RGA inhibits plant growth and enhance the salinity
576 tolerance.
577 ≥ 30 seedlings are analyzed for each sample in (B) and (C). Data presented in (E) and (F) are
578 means of three independent experiments with S.D. * and ** indicate $P < 0.05$ and $P < 0.01$,
579 respectively (One-way ANOVA test).
580

STAR★METHODS

KEY RESOURCES TABLE

REAGENT or RESOURCE	SOURCE	IDENTIFIER
Antibodies		
HRP-linked anti-biotin	Cell Signaling Technology	Cat#7075
Mouse monoclonal anti-GFP	Abmart	Cat# M20004L
Mouse monoclonal anti-GST	Abgent	Cat # AM1011a
Mouse monoclonal anti-His	CMCTAG	Cat # AT0025
Mouse monoclonal anti-tubulin	Sigma-Aldrich	Cat# T5168
Rabbit polyclonal anti-HA	Abgent	Cat# AP1012a
Mouse monoclonal anti-FLAG® M2-peroxidase (HRP) antibody	Sigma-Aldrich	Cat# A8592
Mouse polyclonal anti-RGA	This paper	N/A
Bacterial and Virus Strains		
E. coli DH5	TransGen Biotech	Cat# CD201
E. coli BL21	TransGen Biotech	Cat# CD901
Agrobacterium tumefaciens GV3101	Biomed	Cat# BC304
Chemicals, Peptides, and Recombinant Proteins		
His-SLY1	This paper	N/A
His-GID1a	This paper	N/A
His-GID1c	This paper	N/A
His-RGA Nter	This paper	N/A
GST^{4CS}	(Feng et al., 2013)	N/A
GST^{4CS}-RGA	This paper	N/A
GST^{4CS}-RGA^{C374S}	This paper	N/A
GST^{4CS}-GAI	This paper	N/A
GST^{4CS}-RGL1	This paper	N/A
GST^{4CS}-RGL2	This paper	N/A
GST^{4CS}-RGL3	This paper	N/A
S-nitrosoglutathione (GSNO)	Sigma-Aldrich	Cat# N4148
Sodium nitroprusside (SNP)	Sigma-Aldrich	Cat# 71778
Biotin-HPDP	Thermo Scientific	Cat# 21341
Biotin-maleimide	Sigma-Aldrich	Cat# B1267
Glutathione	Sigma-Aldrich	Cat# G4251
Methyl methanethiosulfonate (MMTS)	Thermo Scientific	Cat# 23011
Neocuproine	Sigma-Aldrich	Cat# N1501

Sodium ascorbate	Sigma-Aldrich	Cat# A7631
Gibberellic acid (GA_3)	TCI	Cat# G0029
Paclobutrazol	Sigma-Aldrich	Cat# 46046
Protease Inhibitor Cocktail	Sigma-Aldrich	Cat# P9599
Trypsin	Promega	Cat# V5280
Critical Commercial Assays		
Ni-NTA resin	QIAGEN	Cat# 30210
Glutathione Sepharose	GE	Cat# 17-0756-01
High Capacity Neutravidin Agarose Resin	Thermo Scientific	Cat# 29202
Anti-FLAG® M2 Affinity Gel	Sigma-Aldrich	Cat# A2220
Zeba Spin Desalting Columns	Thermo Scientific	Cat# 89883
Experimental Models: Organisms/Strains		
Arabidopsis: gsnor1-3	(Feechan et al., 2005)	GABI_315D11
Arabidopsis: nox1	(He et al., 2004)	N/A
Arabidopsis: *rga*	This paper	SALK_089146
Arabidopsis: *gai-t6 rga-24*	(King et al., 2001)	N/A
Arabidopsis: *gai-t6 rga-t2 rgl1-1 rgl2-1*	(Achard et al., 2006)	N/A
Arabidopsis: pRGA:: *GFP-RGA*	(Silverstone et al., 2001)	N/A
Arabidopsis: pRGA:: *GFP-RGA* (*pER8*)	This paper	N/A
Arabidopsis: pRGA:: *GFP-RGA*^{C374S}	This paper	N/A
Oligonucleotides		
Primers for cloning, PCR and genotyping	This paper (see Table S1)	N/A
Recombinant DNA		
pET28a-SLY1	This paper	N/A
pET28a-GID1a	This paper	N/A
pET28a-GID1c	This paper	N/A
pET28a-RGA Nter	This paper	N/A
pGST^{4CS}	(Feng et al., 2013)	N/A
pGST^{4CS}-RGA	This paper	N/A
pGST^{4CS}-RGA^{C374S}	This paper	N/A
pGST^{4CS}-GAI	This paper	N/A
pGST^{4CS}-RGL1	This paper	N/A
pGST^{4CS}-RGL2	This paper	N/A
pGST^{4CS}-RGL3	This paper	N/A
pWM101-FLAG-RGA	This paper	N/A
pWM101-FLAG-RGA^{C374S}	This paper	N/A
pWM101-HA-SLY1	This paper	N/A
pER8-pRGA:: GFP-RGA	This paper	N/A
pER8-pRGA:: GFP-RGA ^{C374S}	This paper	N/A

Software and Algorithms		
ImageJ	NIH	http://imagej.nih.gov/ij/

LEAD CONTACT AND MATERIALS AVAILABILITY

Further information and requests for resources and reagents should be directed to and will be fulfilled by the Lead Contact, Jianru Zuo (jrzuo@genetics.ac.cn)

EXPERIMENTAL MODEL AND SUBJECT DETAILS

Columbia-0 (Col-0) and Landsberg *erecta* (L*er*) accessions of *Arabidopsis* was used in this study. The *gsnor1-3* mutant seeds (Feechan et al., 2005) were provided by Gary Loake. The *nox1* mutant seeds (He et al., 2004) were provided by Yikun He. The *gai-t6 rga-24*, *gai-t6 rga-t2 rgl1-1 rgl2-1*, and *pRGA*::*GFP-RGA* transgenic line (L*er* background) (Achard et al., 2006; King et al., 2001; Silverstone et al., 2001) were provided by Xiangdong Fu. The *rga* (SALK_089146) mutant was obtained from ABRC. Generation of transgenic *Arabidopsis* plants was carried out by *Agrobacterium*-mediated transformation (Bechtold and Pelletier, 1998). The *pRGA*:: *GFP-RGA* and *pRGA*::*GFP-RGA*^{C374S} were introduced into *gai-t6 rga-24* plants. T2 or subseqent generations of transgenics that are homozygous for a single insertion were used for all studies. At least two independent transgenic lines are analyzed. Unless specified otherwise, no apparent phenotype was observed in these transgenic plants under normal growth conditions.

Seeds were sterilized and sown on 1/2 MS medium agar plates with 1% sucrose. The seeds were imbibed at 4°C for 2 days, and then cultured at 22°C under 16/8 h light/dark.

METHODS DETAILS

Plasmid construction

The coding sequence of *RGA* was inserted into the *BamH*I/*Sal*I sites of pGST^{4CS}, a modified pGEX4T1 vector, to generate pGST^{4CS}-RGA. The pGST^{4CS}-GAI, pGST^{4CS}-RGL1, pGST^{4CS}-RGL2, and pGST^{4CS}-RGL3 constructed were generated in a similar way. The coding sequences of *SLY1* and *GID1a* were inserted into the *BamH*I/*Hind*III sites and *BamH*I/*Sal*I sites,

611 respectively, to produce pET28a-SLY1 and pET28a-GID1a. The pET28a-GID1c and pET28a-
612 RGA Nter vectors were generated in a similar way.

613 Putative promoter sequences and the coding regions of *RGA* were separately amplified and
614 appropriate restriction sites were introduced during PCR. The promoter fragment was digested
615 with *Xho*I/*Nco*I, and cloned into pSK-GFP with the same sites to generate pSK-pRGA::GFP.
616 Fragments of *pRGA*::*GFP* and *RGA* coding regions were digested with *Xho*I/*Pst*I and *Pst*I/*Spe*I,
617 respectively, and then cloned into the *Xho*I/*Spe*I sites of a pER8 binary vector (Zuo et al., 2000)
618 to generate pER8- pRGA::GFP-RGA.

619 The coding sequences of *RGA* and *SLY1* were PCR-amplified and in-frame fused to an
620 FLAG or HA tag to yield pSK-FLAG-RGA and pSK-HA-SLY1, respectively. *FLAG-RGA* and
621 *HA-SLY1* were PCR-amplified and ligated to pMW101 at *Kpn*I/*Sal*I and *Kpn*/*Pst*I under the
622 control of a 35S promoter, respectively, to generate pWM101-FLAG-RGA and pWM101-HA-
623 SLY1.

624 The BiFC expression vectors pCAMBIA1300-YNE-RGA and pCAMBIA1300-YCE-SLY1
625 were constructed by a approach described previously (Chen et al., 2020).

626 Site-directed mutagenesis was performed using the Easy Mutagenesis System (TransGen
627 Biotech, Beijing) according the manufacturer's instructions. Primers used for the mutagenesis are
628 listed in Table S1.

629 All constructs were verified by extensive restriction digestion and DNA sequencing analysis.
630 All PCR-related primers used in this study are listed in Table S1.

631 **Expression and purification of recombinant proteins**

632 The pET28a-SLY1, pET28a-GID1a, pET28a-GID1c, pET28a-RGA Nter, pGST^{4CS}-RGA,
633 pGST^{4CS}-RGA ^{C374S} , pGST^{4CS}-GAI, pGST^{4CS}-RGL1, pGST^{4CS}-RGL2, and pGST^{4CS}-RGL3
634 expression vectors were transformed into *Escherichia coli* strain BL21 (DE3). Expression and
635 purification of the recombinant proteins were carried out following the manufacturer's
636 instructions.

637 **Generation of antibodies and immunoblotting**

Anti-tubulin (Sigma-Aldrich, Cat #T5168), anti-GST (Abgent, Cat #AM1011a), anti-His (CMCTAG, Cat #AT0025), anti-GFP (Abmart, Cat#M20004L), anti-HA (Abgent, Cat #AP1012a) and anti-FLAG (Sigma-Aldrich, Cat #A8592) antibodies were obtained from commercial sources. RGA-specific antibodies were generated by immunizing mice with *Escherichia coli*-expressed N-terminal of RGA (His-RGA Nter). Total protein was extracted and no cross-reaction was observed in the *rga* mutant compared with Col-0 (Supplemental Figure 2C). Immunoblotting was carried out as previously described (Chen et al., 2009). Quantification of the immunoblot was performed using NIH ImageJ (version 1.44p; http://imagej.nih.gov/ij/).

Bimolecular fluorescence complementation analysis

Bimolecular fluorescence complementation (BiFC) assays were performed as described (Chen et al., 2020). The *Nicotiana benthamiana* leaves were injected with agrobacteria cultures containing expression vectors and cultured for additional two days. 300 μM GSNO was sprayed on the surface of the tobacco leaves for 2 hours. The leaves were then excised and observed under a confocal microscope.

In vitro pull down

GST^{4CS}-tagged RGA or RGA^{C374S} recombinant proteins were incubated with indicated concentrations of GSH or GSNO in HEN buffer (250mM Hepes, pH 7.7, 1mM EDTA , 1 mM neocuproine) for 30 min. Free GSNO or GSH was removed using Zeba Spin Desalting Columns (Thermo, Cat #: 89883). 1 μg GST^{4CS} and 2 μg GST^{4CS}-tagged RGA or RGA^{C374S} recombinant proteins immobilized on Glutathione Sepharose. Immobilized beads were incubated with 1 μg His-tagged recombinant proteins in PBS-140N buffer (137 mM NaCl, 2.7 mM KCl, 10 mM Na_2PO_4, 2 mM KH_2PO_4, pH 7.4, 0.5% IGEPAL CA-630) for 1 hr at 4°C. For His-GID1a and His-GID1c, 10 μM GA_3 was added. The supernatant was removed after centrifugation at 800 rpm, and the beads were washed six times with precooled PBS-140N buffer. The resin-retained proteins were analyzed by western blot analysis using anti-His or anti-GST antibodies as indicated.

Co-immunoprecipitation

Co-immunoprecipitation experiments were performed as previously described (Ren et al., 2013) with modifications. pWM101-FLAG-RGA, pWM101-FLAG-RGA^{C374S}, and pWM101-HA-SLY1 constructs were transiently expressed in tobacco leaves by agrobacterium-mediated infiltration (strain GV3101). After cultured for additional three days, tobacco leaves were incubated with 10 μM paclobutrazol for 3 hours and treated with 300 μM SNP for another 1 hour. Tobacco leaves were then ground in liquid nitrogen and extracted in IP buffer (50 mM Tris-HCl, pH 7.4, 150 mM NaCl, 5% glycerol, 0.1% IGEPAL CA-630) supplemented with Protease Inhibitor Cocktail. Samples were centrifuged at 13,000 rpm for 20 min at 4°C and the supernatant was collected. Proteins were incubated with anti-FLAG® M2 affinity gel (Sigma, Cat # A2220) for 2 hours at 4°C. The gel were washed 6 times with IP buffer and proteins were then eluted and analyzed by immunoblotting.

In vitro *S*-nitrosylation assay

Analysis of *in vitro S*-nitrosylation was performed essentially as described (Chen et al., 2020). Approximately 10 μg of GST^{4CS}-tagged RGA or RGA^{C374S} recombinant proteins were incubated with GSNO or GSH at a final concentration of 200 μM in the dark for 30 min. Protein was precipitated by adding three volumes of cold acetone. The pellet was washed three times with 70% acetone and resuspended in 200 μL blocking buffer 1 (250 mM Hepes, pH 7.7, 4 mM EDTA, 1 mM neocuproine, 2.5% SDS and 200 mM *S*-methylmethane thiosulfonate). After incubation at 50°C for 40 min, protein was precipitated by adding three volumes of acetone and washed with 70% acetone. The pellet is dissolved in 80 μL HENS buffer (250 mM Hepes, pH 7.7, 4 mM EDTA, 1 mM neocuproine, 1% SDS), followed by addition of 10 μL 500 mM sodium ascorbate and 10 μL of 4 mM biotin-HPDP. The reaction was run for 1 hr at room temperature. Samples were separated by SDS-PAGE and analyzed by immunoblotting using an anti-biotin antibody (Cell Signaling Technology, Cat#7075).

In vivo *S*-nitrosylation assay

Analysis of *in vivo S*-nitrosylation was performed as described (Feng et al., 2013) with minor modifications. In brief, two-week-old seedlings were ground in liquid nitrogen and extracted

692 HEN/RIPA buffer (250 mM Hepes, pH 7.7, 1mM EDTA, 0.1 mM neocuproine, 1% Triton X-100,
693 protease inhibitor cocktail, 0.1% SDS and 1% sodium deoxycholate). 300 μg protein was
694 incubated with blocking buffer at 50°C for 40 min. Protein was precipitated with cold acetone.
695 The pellet was washed three times with 70% acetone and resuspended in 240 μL of HENS buffer
696 followed by addition of 30 μL of 500 mM sodium ascorbate and 30 μL of 4 mM biotin-HPDP.
697 The reaction was run for 1 hr at room temperature. Protein was precipitated with cold acetone,
698 washed three times with 70% acetone and resuspended in 300 μL HENS buffer. After being
699 neutralized with 900 μL of neutralization buffer (25 mM HEPES, pH 7.7, 100 mM NaCl, 1 mM
700 EDTA, and 0.5% Triton X-100), the sample was mixed with 40 μL of streptavidin beads (Thermo
701 Scientific, Cat #29202) and incubated at 4°C overnight. The beads were washed six times with
702 washing buffer (25 mM HEPES, pH 7.7, 600 mM NaCl, 1 mM EDTA, and 0.5% Triton X-100).
703 The proteins were then eluted and analyzed by immunoblotting.

704 **Mass spectrometric analysis of *S*-nitrosylation residues**

705 Mass spectrometric identification of *S*-nitrosylated cysteine residues was carried out as described
706 (Chen et al., 2020). Approximately 30 μg GST^{4CS}-RGA recombinant proteins were labeled with
707 biotin-maleimide (Sigma-Aldrich, Cat#B1267). The biotinylated protein was digested with
708 Trypsin (Promega, Cat#V5280) in gel. The Trypsin-digested sample was analyzed by LC-MS/MS
709 using a Thermo Fisher Finnigan linear ion trap quadrupole mass spectrometer in line with a
710 Thermo Fisher Finnigan Surveyor MS Pump Plus HPLC system. The raw data was searched
711 against the GST^{4CS}-RGA protein sequence using pFIND searching software. Cysteine
712 biotinylation (451.200 Da), cysteine carbamidomethylation (57 Da), and methionine oxidation
713 (15.995 Da) were included in the search as the variable modifications.

714

715 **QUANTIFICATION AND STATISTICAL ANALYSIS**

716 For quantification analyses, the mean and SD were calculated and compared to control and
717 significance (*P* value) was determined using the two-tailed Student's *t*-test or one-way ANOVA
718 test (specified in Figure legends). All experiments were repeated at least 3 times, and

719 representative results are shown.

720

721

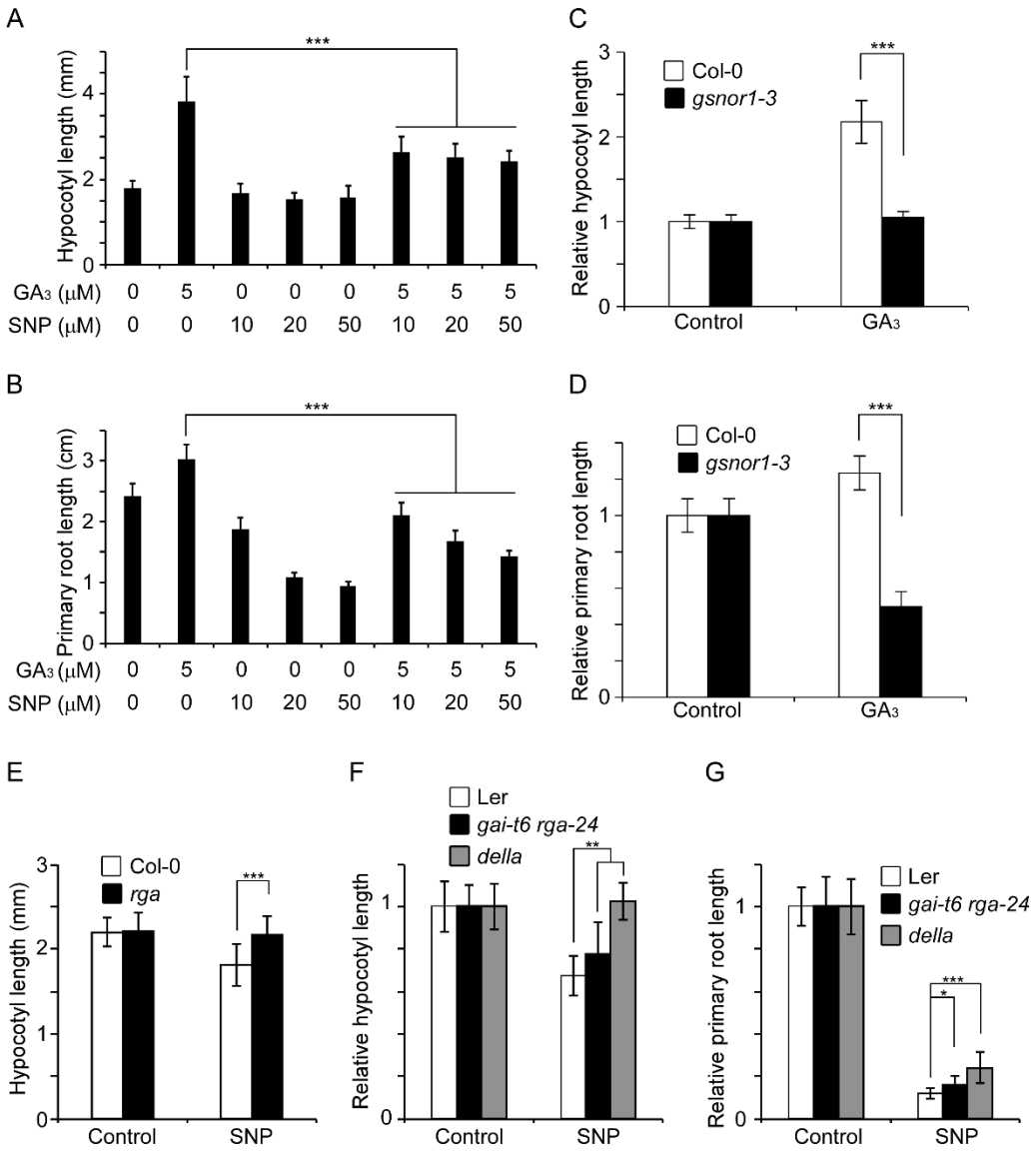

722

723

724 **Figure 1. Nitric oxide antagonizes gibberellin-promoted root and hypocotyl elongation, see**

725 **also Supplemental Figure S1 and S2**

726 (A and B) Hypocotyl length (A) and primary root length (B) of 7-day-old Col-0 seedlings treated

727 with the indicated concentrations of gibberellic acid (GA_3) and sodium nitroprusside (SNP).

728 (C and D) Hypocotyl length (C) and primary root length (D) of 7-day-old Col-0 and *gsnor1-3*

729 seedlings treated with 5 μM GA_3.

730 (E) Hypocotyl length of 7-day-old Col-0 and *rga* seedlings treated with 20 μM SNP.

731 (F and G) Hypocotyl length (F) and primary root length (G) of 7-day-old Col-0, *gai-t6 rga-24*
732 and *della* (*gai-t6 rga-t2 rgl1-1 rgl2-1*) seedlings treated with 20 μM SNP.
733 In each experiment, 30 seedlings were analyzed. *, **, and *** indicate $P < 0.05$, $P < 0.01$, and P
734 < 0.001 (one-way ANOVA test), respectively.
735

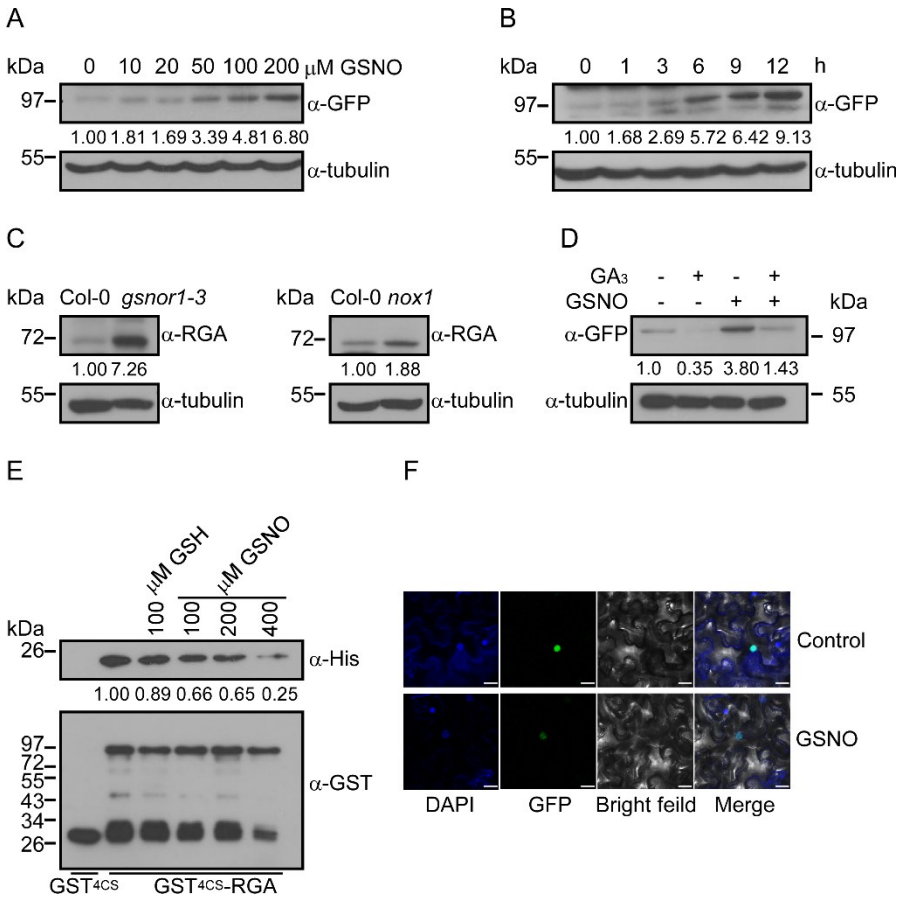

Figure 2. Nitric oxide inhibits gibberellin-promoted RGA degradation, see also Supplemental Figure S3, S4 and Table S1

(A and B) Immunoblotting analysis of GFP-RGA proteins in 7-day-old *pRGA*::*GFP-RGA* transgenic seedlings treated with indicated concentrations of GSNO for 6 hours (A) and 300 μM GSNO for the indicated times (B) by using an anti-GFP antibody. Immunoblotting with an anti-tubulin antibody is served as a loading control. Quantification of GFP-RGA is shown below the blot.

(C) Immunoblotting analysis of RGA proteins in 7-day-old Col-0, *gsnor1-3*, and *nox1* seedlings by using an anti-RGA antibody. Quantification of RGA is shown below the blot.

(D) Immunoblotting analysis of GFP-RGA proteins in 7-day-old *pRGA*::*GFP-RGA* transgenic seedlings treated with or without 300 μM GSNO and 0.5 μM GA_3 for 6 hours using an anti-GFP antibody. Quantification of GFP-RGA is shown below the blot.

(E) Analysis of the interaction of SLY1 and RGA1 recombinant proteins with a pull-down assay. GST^{4CS}-RGA protein was treated with the indicated concentrations of GSNO or GSH prior to the incubation with His-SLY1. Quantification of the His-SLY1 level is shown below the blot.

(F) Bimolecular fluorescence complementation (BiFC) analysis of co-localization of YNE-RGA1 and YCE-SLY1 fusion proteins in transiently expressed in tobacco leaves sprayed with 300 μM GSNO. Bar, 20 μm.

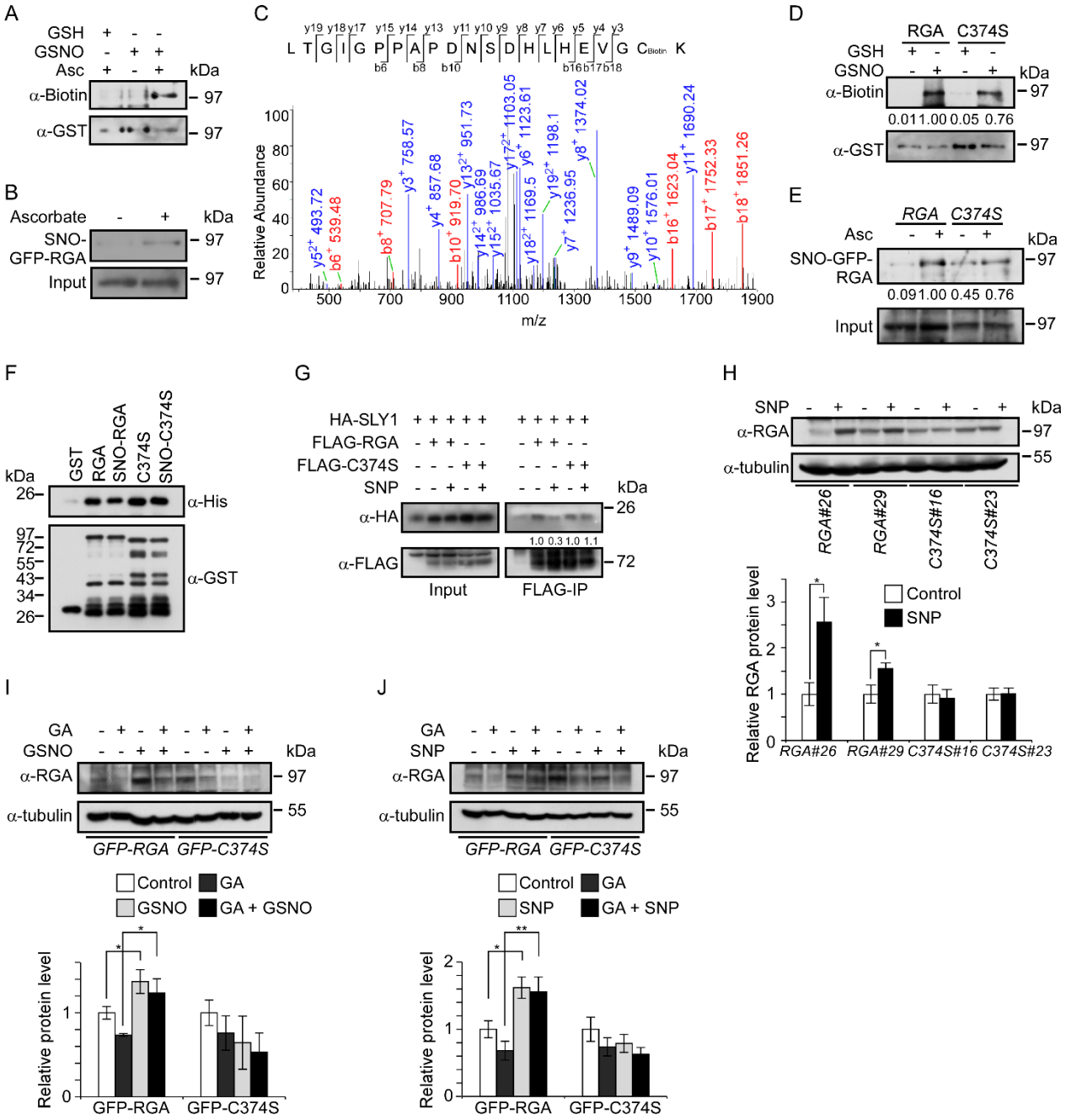

Figure 3. *S*-nitrosylation at Cys-374 modulates RGA stability, see also Supplemental Figure S4 and S5, Table S1 and Table S2

(A) Analysis of *S*-nitrosylated GST^{4CS}-RGA recombinant protein treated with GSNO by an in vitro *S*-nitrosylation assay. Treatment with GSH and without sodium ascorbate (Asc) are served

765 as negative controls.
766 (B) Analysis of *S*-nitrosylated GFP-RGA protein in *pRGA*::*GFP-RGA* transgenic seedlings by an
767 in vivo *S*-nitrosylation assay. The sample without Asc treatment is served as a negative control.
768 (C) Liquid chromatography tandem-mass (LC-MS/MS) spectrum of trypsin-digested and biotin-
769 charged RGA peptides. The b- and y-type product ions are indicated, which identified Cys-374 as
770 an *S*-nitrosylated residue.
771 (D) Analysis of *S*-nitrosylated GST^{4CS}-RGA (RGA) and GST^{4CS}-RGA^{C374S} (C374S) recombinant
772 proteins treated with GSNO by an in vitro *S*-nitrosylation assay. Treatment with GSH is served as
773 negative controls. Quantification of the *S*-nitrosylation level of GST^{4CS}-RGA and GST^{4CS}-
774 RGA^{C374S} is shown below the blot.
775 (E) Analysis of *S*-nitrosylated GFP-RGA and RGA^{C374S} (C374S) proteins in planta by an in vivo
776 *S*-nitrosylation assay. The sample without Asc treatment is served as a negative control.
777 Quantification of the *S*-nitrosylation level of RGA and RGA^{C374S} is shown below the blot.
778 (F) Analysis of the interaction of RGA, RGA^{C374S} and SLY1 recombinant proteins with a pull-
779 down assay. GST^{4CS}-RGA and GST^{4CS}-RGA^{C374S} was treated with 300 μM GSNO to generate *S*-
780 nitrosylated proteins prior to the incubation with His-SLY1.
781 (G) Analysis of the interaction of HA-SLY1, FLAG-RGA and FLAG-RGA^{C374S} (FLAG-C374S)
782 proteins by a co-immunoprecipitation assay. The *HA-SLY1* and *FLAG-RGA* fusion genes under
783 the control of the 35S promoter were transiently expressed in tobacco leaves that were incubated
784 with or without 300 μM SNP for 1 hour. Protein extracts were used for Co-IP and analyzed by
785 immunoblotting using anti-HA and -FLAG antibodies. Quantification of HA-SLY1 is shown
786 below the blot. And protein level of HA-SLY1 that interacts with FLAG-RGA and FLAG-C374S
787 without SNP treatment is set as 1.0, respectively.
788 (H) Immunoblotting analysis of GFP-RGA proteins in *gai-t6 rga-24* transgenic seedlings of the
789 indicated genotypes treated with 300 μM SNP for 6 hours using an anti-RGA antibody.
790 Quantification of the GFP-RGA and GFP-RGA^{C374S} protein levels is shown below the blot.
791 Protein levels of GFP-RGA and GFP-RGA^{C374S} without treatment are set as 1.0, respectively.

(I) Immunoblotting analysis of GFP-RGA and GFP-RGA^{C374S} proteins in 7-day-old *pRGA*::*GFP-RGA*, *pRGA*::*GFP-RGA*^{C374S} transgenic seedlings treated with or without 300 μM GSNO and 0.5 μM GA_3 for 6 hours by using an anti-RGA antibody. Quantification of the GFP-RGA and GFP-RGA^{C374S} protein levels is shown below the blot. Protein levels of GFP-RGA and GFP-RGAC374S without treatment are set as 1.0, respectively.

(J) Immunoblotting analysis of GFP-RGA and GFP-RGA^{C374S} proteins in 7-day-old *pRGA*::*GFP-RGA*, *pRGA*::*GFP-RGA*^{C374S} transgenic seedlings treated with or without 300 μM SNP, and 0.5 μM GA_3 for 6 hours by using an anti-RGA antibody. Quantification of the GFP-RGA and GFP-RGA^{C374S} protein levels is shown below the blot. Protein levels of GFP-RGA and GFP-RGA^{C374S} without treatment are set as 1.0, respectively.

Data presented in (H)-(J) are means of three independent experiments with S.D. * and ** indicate $P < 0.05$ and $P < 0.01$, respectively (One-way ANOVA test).

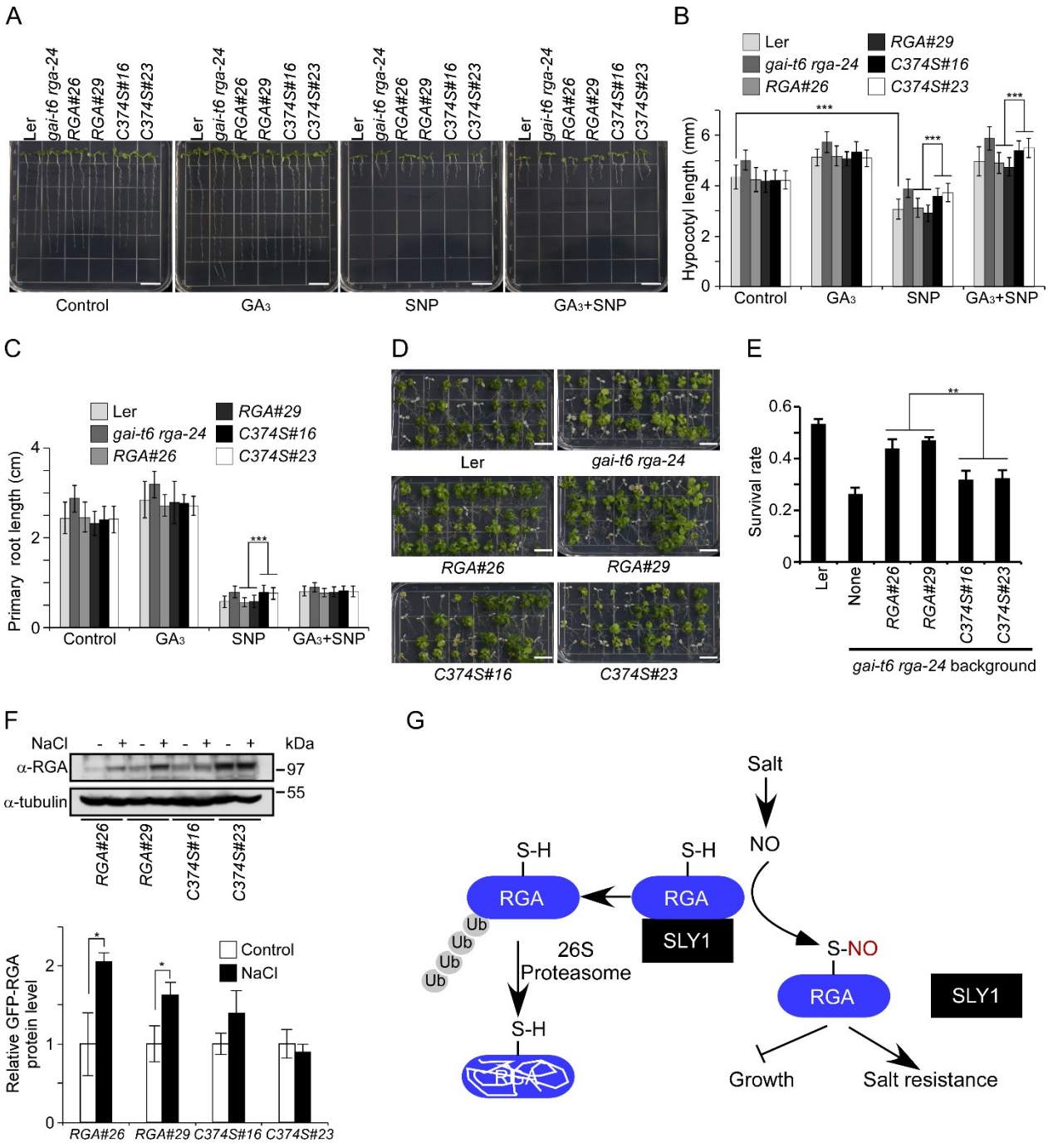

Figure 4. *S*-nitrosylation of RGA balances plant growth and salinity tolerance, see also Figure S4 and Supplemental Table S2

(A) Ten-day-old seedlings of the indicated genotypes treated with 50 μM SNP or 5 μM GA_3. Bar, 1 cm.

(B) and (C) Analysis of hypocotyl length (B) and primary root length (C) of transgenic seedlings of the indicated genotypes treated with 50 μM SNP or 5 μM GA_3 for 10 days.

(D) Five-day-old seedlings of the indicated genotypes on 1/2MS medium were transferred to the medium containing 125 mM NaCl. Photos were taken 2 weeks post the transfer. Bar, 1 cm.

(E) Analysis of the survival rate of transgenic seedlings of the indicated genotypes shown in (D).

(F) Immunoblotting analysis of GFP-RGA proteins in *gai-t6 rga-24* transgenic seedlings of the indicated genotypes treated with 150 mM NaCl for 6 hours using an anti-RGA antibody. Quantification of the GFP-RGA and GFP-RGA^{C374S} protein levels is shown below the blot.

(G) A proposed model illustrating the function of *S*-nitrosylation of RGA. Under normal growth conditions, SLY1 interacts with RGA, which leads to the polyubiquitination and degradation of RGA via the 26S proteasome pathway. High salt induces the NO burst, which subsequently induces the *S*-nitrosylation of RGA. The *S*-nitrosylation inhibits the RGA-SLY1 interaction and enhances the stability of RGA. Accumulating RGA inhibits plant growth and enhance the salinity tolerance.

≥ 30 seedlings are analyzed for each sample in (B) and (C). Data presented in (E) and (F) are means of three independent experiments with S.D. * and ** indicate $P < 0.05$ and $P < 0.01$, respectively (One-way ANOVA test).

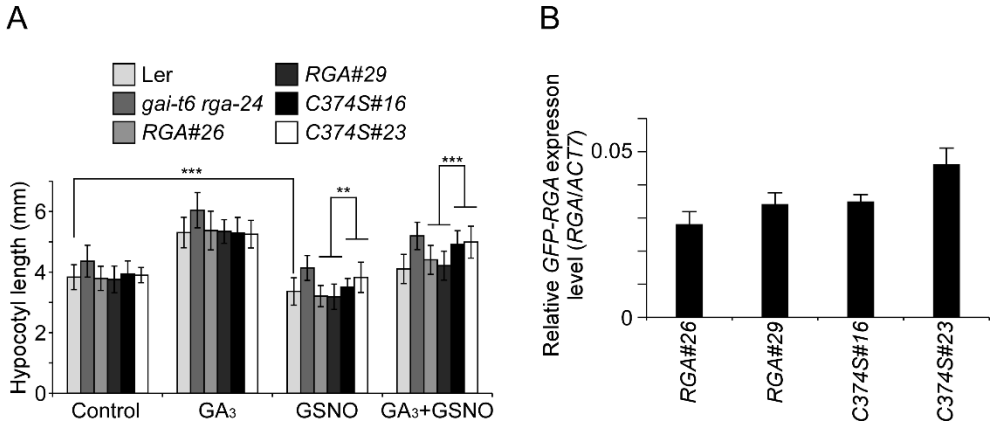

Figure S1 *S*-nitrosylation of RGA modulates plant growth, related to Figure 1 and 4

(A) Analysis of hypocotyl length of transgenic seedlings of the indicated genotypes treated with 300 μM GSNO or 5 μM GA_3 for 10 days. Thirty seedlings were analyzed. *, **, and *** indicate $P < 0.05$, $P < 0.01$, and $P < 0.001$ (one-way ANOVA test), respectively.

(B) Analysis of the expression of *GFP-RGA* by qRT-PCR in 7-day-old transgenic seedlings.

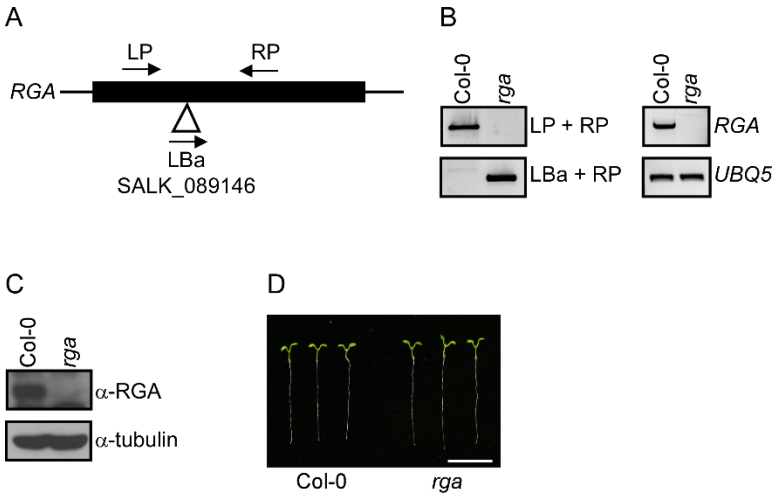

Figure S2. Characterization of *rga* mutant, related to Figure 1

(A) The gene structure is indicated with exons represented by boxes and UTRs represented by lines. The position of T-DNA is indicated with open triangle.

(B) Genotyping of *rga* mutant.

(C) Analysis of *RGA* expression by RT-PCR. *RGA* expression in Col-0 and the *rga* mutant is shown. *UBQ5* was used as loading control.

(D) Analysis of RGA protein level in Col-0 and the *rga* mutant. Total protein was extracted from 7-day-old seedlings and probed with anti-RGA and anti-tubulin antibodies.

(E) Seven-day-old seedlings of Col-0 and *rga* mutant. Bar, 1 cm.

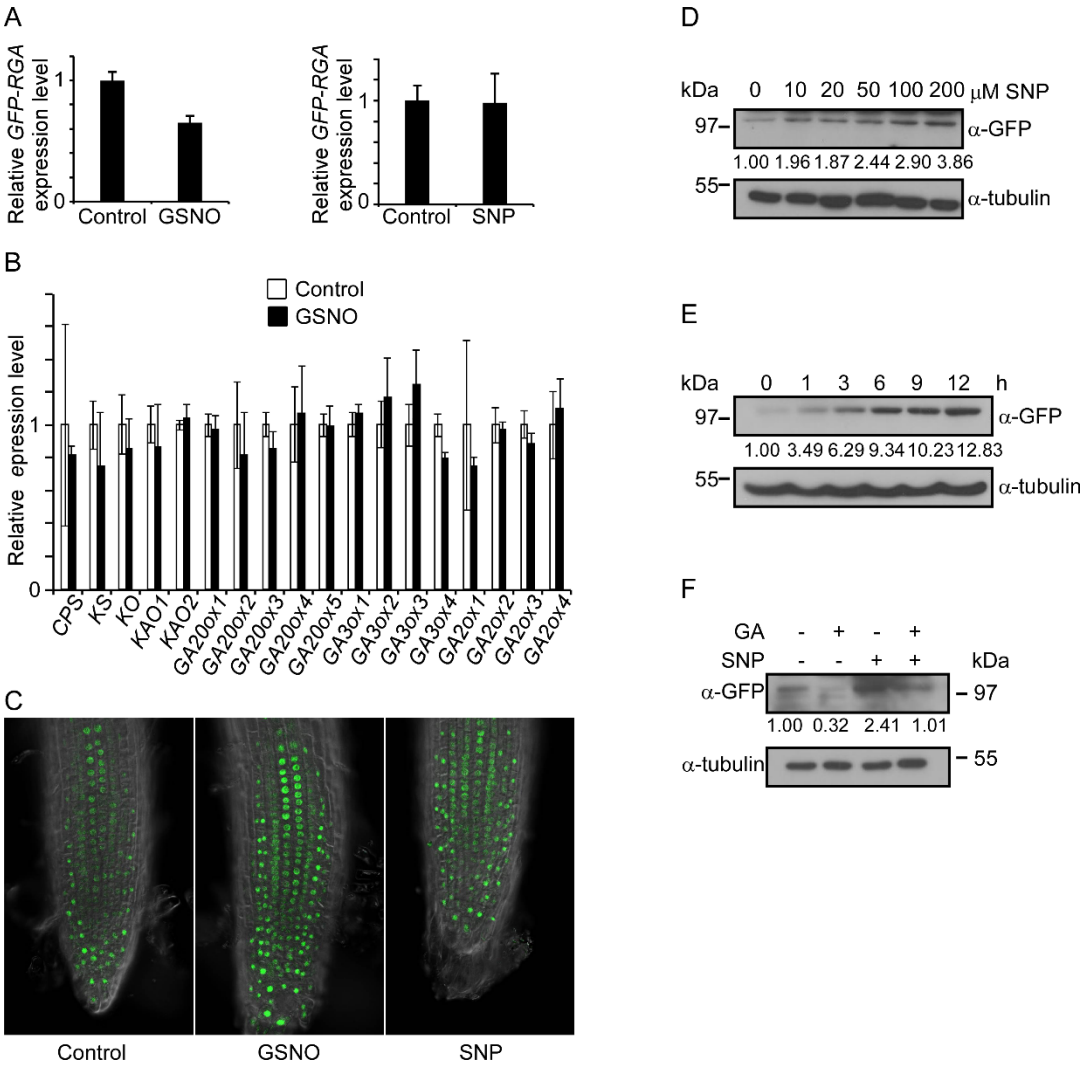

Figure S3. NO inhibits GA-promoted RGA degradation, related to Figure 2

(A) Analysis of the expression of *GFP-RGA* by qRT-PCR in 7-day-old *pRGA*::*GFP-RGA* transgenic plants treated with 300 μM GSNO or SNP for 6 hours.

(B) Analysis of the expression of GA biosynthesis genes by qRT-PCR in 7-day-old Col-0 seedlings treated with 300 μM GSNO for 6 hours.

(C) Confocal microscopic images of root tips derived from *pRGA*::*GFP-RGA* transgenic seedlings treated with 300 μM GSNO or SNP.

(D and E) Immunoblotting analysis of GFP-RGA proteins in 7-day-old *pRGA*::*GFP-RGA*

transgenic plants treated with indicated concentrations of SNP for 6 hours (D) and 300 μM SNP for indicated times (E) using an anti-GFP antibody, and immunoblotting with an anti-tubulin antibody is served as loading control. Quantification of GFP-RGA is shown below the blot.

(F) Immunoblotting analysis of GFP-RGA proteins in 7-day-old *pRGA*::*GFP-RGA* transgenic plants treated with or without 300 μM SNP or 0.5 μM GA for 6 hours using an anti-GFP antibody. Quantification of GFP-RGA is shown below the blot.

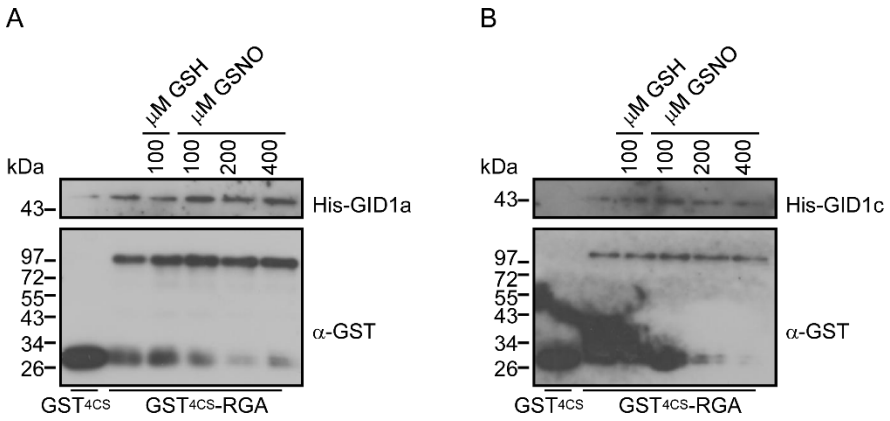

Figure S4 RGA-GID1 interaction is not regulated by NO, related to Figure 2

(A and B) Analysis of the interaction of His-GID1a (A), His-GID1c (B) with GST^{4CS}-RGA recombinant proteins with a GST pull-down assay. GST^{4CS} -RGA protein was treated with indicated concentrations of GSNO or GSH before incubated with His-GID1a or His-GID1c.

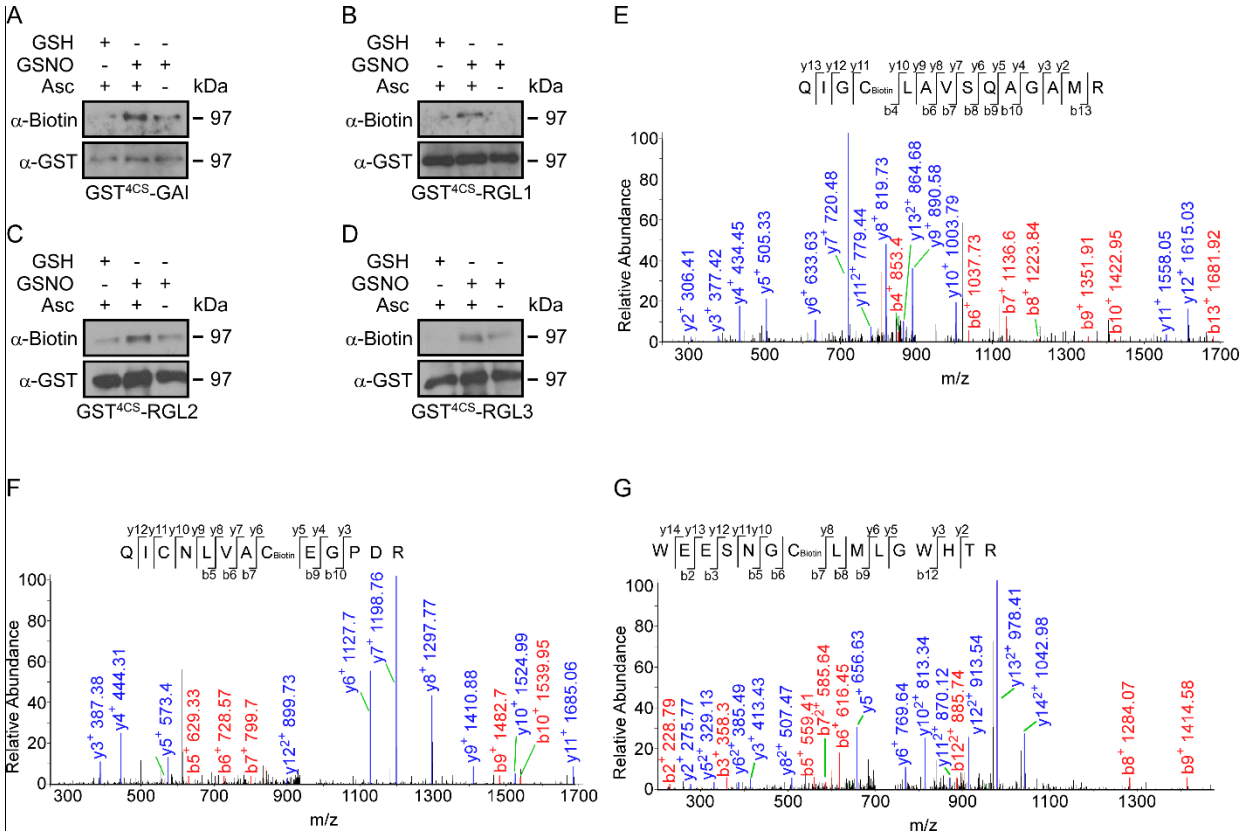

Figure S5 DELLA proteins are *S*-nitrosylated in vitro, related to Figure 3

(A to D) Analysis of *S*-nitrosylated GST^{4CS}-GAI (A), GST^{4CS}-RGL1 (B), GST^{4CS}-RGL2 (C), and GST^{4CS}-RGL3 (D) recombinant proteins treated with GSNO by an in vitro *S*-nitrosylation assay. Treatment with GSH and without sodium ascorbate (Asc) are served as negative controls.

(E to G) Liquid chromatography tandem-mass (LC-MS/MS) spectrum of trypsin-digested and biotin-charged RGA peptides. The b- and y-type product ions are indicated, which identified Cys-249 (E), Cys-506 (F), and Cys-564 (G) as an *S*-nitrosylated residues.

892 **Table S1 Primers used in this study, related to Figures 2, 3 and 4.**

893

Primer	Sequences (5' to 3')	Experiments
SLY1 GSTHIS F1	ggatccATGAAGCGCAGTACTACCGACTC	pET28a-SLY1
SLY1 GSTHIS B1	aagcttTTTGGATTCTGGAAGAGGTCTCT	pET28a-SLY1
GID1a GSTHIS F1	ggatccATGGCTGCGAGCGATGAAGTTAATC	pET28a-GID1a
GID1a GSTHIS B1	gtcgacACATTCCGCGTTTACAAACGCCG	pET28a-GID1a
GID1c GSTHIS F1	ggatccATGGCTGGAAGTGAAGAAGTTAATC	pET28a-GID1c
GID1c GSTHIS B1	gtcgacTTGGCATTCTGCGTTTACAAATGC	pET28a-GID1c
RGA GSTHIS F1	GGATCCATGAAGAGAGATCATCACCAAT	pGEX4T14CS-RGA
RGA GSTHIS B1	GTCGACGTACGCCGCCGTCGAGAGTTTC	pGEX4T14CS-RGA
GAI GSTHIS F1	GGATCCATGAAGAGAGATCATCATCATCA	pGEX4T14CS-GAI
GAI GSTHIS B1	GTCGACATTGGTGGAGAGTTTCCAAGCCG	pGEX4T14CS-GAI
RGL1 GSTHIS F1	GGATCCATGAAGAGAGAGCACAACCACC	pGEX4T14CS-RGL1
RGL1 GSTHIS B1	GTCGACTTCCACACGATTGATTCGCCAC	pGEX4T14CS-RGL1
RGL2 GSTHIS F1	GTCGACAAATGAAGAGAGGATACGGAGAA	pGEX4T14CS-RGL2
RGL2 GSTHIS B1	CGGCCGGGCGAGTTTCCACGCCGAGGTTG	pGEX4T14CS-RGL2
RGL3 GSTHIS F1	GTCGACAAATGAAACGAAGCCATCAAGAA	pGEX4T14CS-RGL3
RGL3 GSTHIS B1	CGGCCGCCGCCGCAACTCCGCCGCTAGTT	pGEX4T14CS-RGL3
RGA NT B2	cagctgTCCTATGACTCCACCAATCTG	pET28a-RGA NT
RGA Pro F1	CTCGAGCATGGTTTTGCATGGAAGAAATA	pER8-pRGA::GFP-RGA
RGA Pro B1	CCATGGTTTTCAGCTATGAGTTTCGATT	pER8-pRGA::GFP-RGA
RGA genome F1	CTGCAGCCAAGAGAGATCATCACCAATTC	pER8-pRGA::GFP-RGA
RGA genome B1	ACTAGTGTACTCTTTGTAACAATAGTTAT	pER8-pRGA::GFP-RGA
RGA 35SFLAG F1	GGTACCATGGATTACAAGGATGACGACGA	pWM101-FLAG-RGA
RGA 35SFLAG B1	GTCGACTCAGTACGCCGCCGTCGAGAGTT	pWM101-FLAG-RGA
SLY1 N MYCHA F1	aagcttAAGCGCAGTACTACCGACTCTGA	pWM101-HA-SLY1
SLY1 N MYCHA B1	ctgcagTTATTTGGATTCTGGAAGAGGTC	pWM101-HA-SLY1
SLY1 35SHA F1	ggtaccATGTATCCTTATGATGTTCCAG	pWM101-HA-SLY1
RGA C374S F1	TGAAGTTGGTaGTAAATTAGCTCAGCT	RGA^{C374S} mutant
RGA C374S B1	GAGCTAATTTACtACCAACTTCATGAAG	RGA^{C374S} mutant
SALK_089146 LP	CCATCACCACCATTCTTTTTC	Identification of *rga*
SALK_089146 RP	TGGACTAAACGAACACCGTTC	Identification of *rga*
ACT7F	GGAACTGGAATGGTGAAGGCTG	qRT-PCR
ACT7B	CGATTGGATACTTCAGAGTGAGGA	qRT-PCR
RGA qRT F1	CGGGACTTCTTCTTCATCATC	qRT-PCR
RGA qRT B1	TGAACATTACTCATCATCGTC	qRT-PCR
CPS qRT F2	CAGTTCTACTAAAACAACAATA	qRT-PCR
CPS qRT B2	CTCTTCACTGCTTCTTTGAAT	qRT-PCR
KS qRT F1	ACCTTCGCTCCTCCGGTTG	qRT-PCR

KS qRT B1	AGATCCATCTTCATGTTGATTAT	qRT-PCR
KO qRT F1	CATTCTCCTTGGCTTTGTTATC	qRT-PCR
KO qRT B1	GTCTCAGTAGAATTGAGGAC	qRT-PCR
KAO1 qRT F1	CTGATGGTGTTGGGATGTTTTG	qRT-PCR
KAO1 qRT B1	TGTTACTATTATACTTGGGTTC	qRT-PCR
KAO2 qRT F1	GCTGAAGAGAGTGAATGTTTG	qRT-PCR
KAO2 qRT B1	CTGTTAGAACTCGCCTACAAG	qRT-PCR
GA20ox1 qRT F1	TTCACCGGACGCTTCTCCAC	qRT-PCR
GA20ox1 qRT B1	GGTAGTAATTCAGTCTCATTATTG	qRT-PCR
GA20ox2 qRT F2	GCAGATTCTCCACTAAGCT	qRT-PCR
GA20ox2 qRT B2	ATGATTGAGCCTCATTATCGAAT	qRT-PCR
GA20ox3 qRT F2	AGTTTCGTCGGGAGATTCT	qRT-PCR
GA20ox3 qRT B2	TCAACCGGAATATTGAATCGC	qRT-PCR
GA20ox4 qRT F2	TCAAGGAGAATCTTCCGTGG	qRT-PCR
GA20ox4 qRT B2	GATACCAAGACTCATTCCAAG	qRT-PCR
GA20ox5 qRT F1	GTGGAATGAGACTTTGACTTTGG	qRT-PCR
GA20ox5 qRT B1	AGGGCTTTCTCTGGCTGC	qRT-PCR
GA3ox1 qRT F2	GCGTCGCTCGTATCGCATC	qRT-PCR
GA3ox1 qRT B2	GCCCAGTTTAAATCTGAAC	qRT-PCR
GA3ox2 qRT F2	TCGTTCTTTAATAAGAAGATGTG	qRT-PCR
GA3ox2 qRT B2	GGATAATGGTTTAGTTGGATA	qRT-PCR
GA3ox3 qRT F2	GAACCGTGACCGGATCATCC	qRT-PCR
GA3ox3 qRT B2	AGCCTCTTCATTTGGCAATCA	qRT-PCR
GA3ox4 qRT F1	GGCTACGGAGAACCTCGAAT	qRT-PCR
GA3ox4 qRT B1	GATCCAGATTTCTCTAGCTTGTG	qRT-PCR
GA2ox1 qRT F2	GGAACAGTAAGATTGGTCGG	qRT-PCR
GA2ox1 qRT B2	CTGTGATCTTCTCCAAAAC	qRT-PCR
GA2ox2 qRT F1	GTACGGTTATGGTAATAAACGG	qRT-PCR
GA2ox2 qRT B1	GCTCTATCCCTAGTTCTTCG	qRT-PCR
GA2ox3 qRT F2	TGGTGACCTTGGCTGGCTTG	qRT-PCR
GA2ox3 qRT B2	CTCAGGCACGAATCACTTTCT	qRT-PCR
GA2ox4 qRT F1	CTCACGAGAAGAAATCTGTCC	qRT-PCR
GA2ox4 qRT B1	GACATGAAGTCCCTCAGCCG	qRT-PCR

894
895
896

897

898 **Table S2 *S*-nitrosylated residues of RGA, related to Figure 3**

899

***S*-nitrosylated residues identified in mass spectrometry**	**Repeat 1**	**Repeat 2**
Cys-249	√	√
Cys-374	√	√
Cys-506	√	
Cys-564	√	√

900

901